The Abdus Salam
International Centre for Theoretical Physics

United Nations
Educational, Scientific and
Cultural Organization

IAEA
International Atomic Energy Agency

2064-6

Joint ICTP/IAEA Advanced School on in-situ X-ray Fluorescence and Gamma Ray Spectrometry

26 - 30 October 2009

X-ray microfluorescence capabilities at Sincrotrone Elettra

D. R. Baker
Ellettra
Trieste
Italy

Elettra microfluorescence beamline:
The X-ray Microprobe

(but not very portable)

What is an X-ray Microprobe?

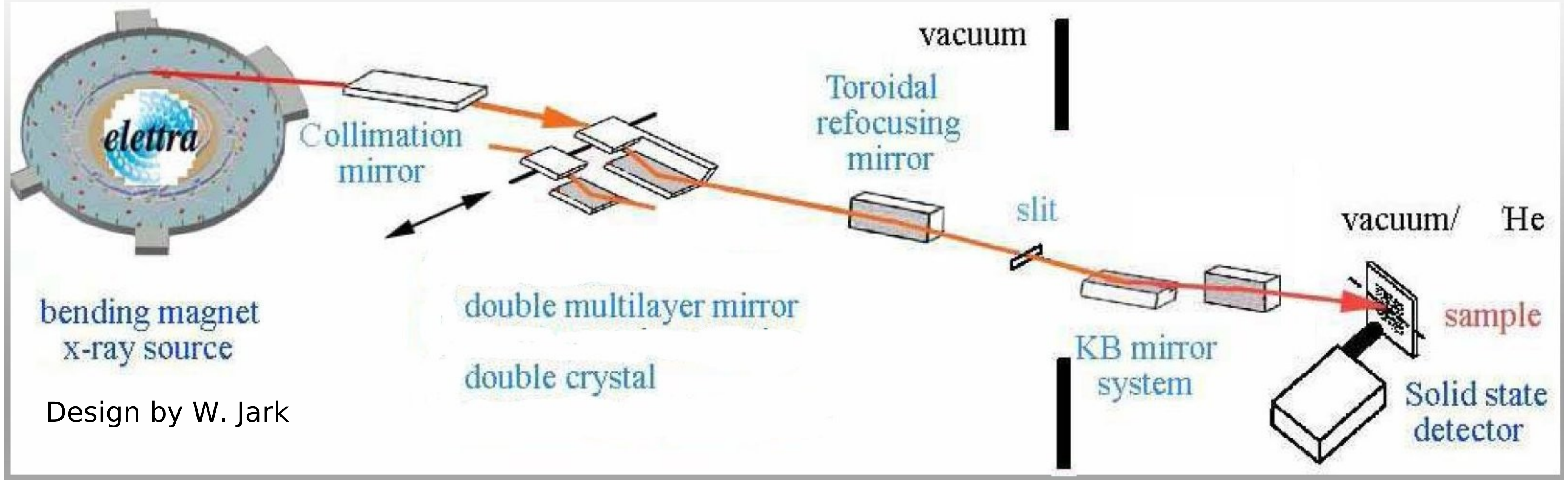

Energy ~ 2 to 14 keV, P to As K_{abs} , Rb to Pt L_{abs}

Focal spot ~ 1 x 1 μm (the smaller the better)

Flux > 10^9 photons/s/0.01% bandwidth

Source to sample: 29 m, Detection limit ~ 1ppm

Beamline Endstation

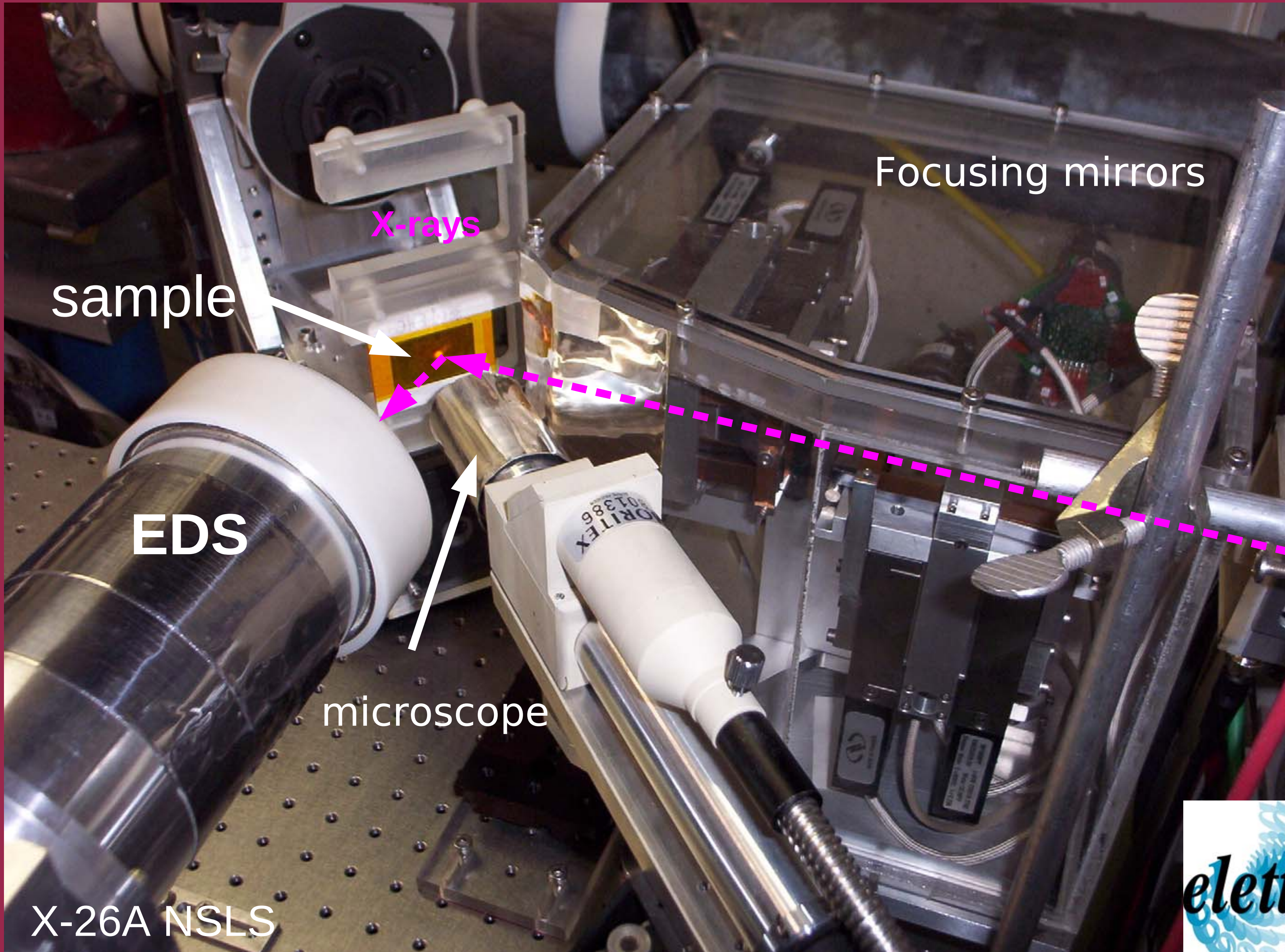

X-ray fluorescence spectrum

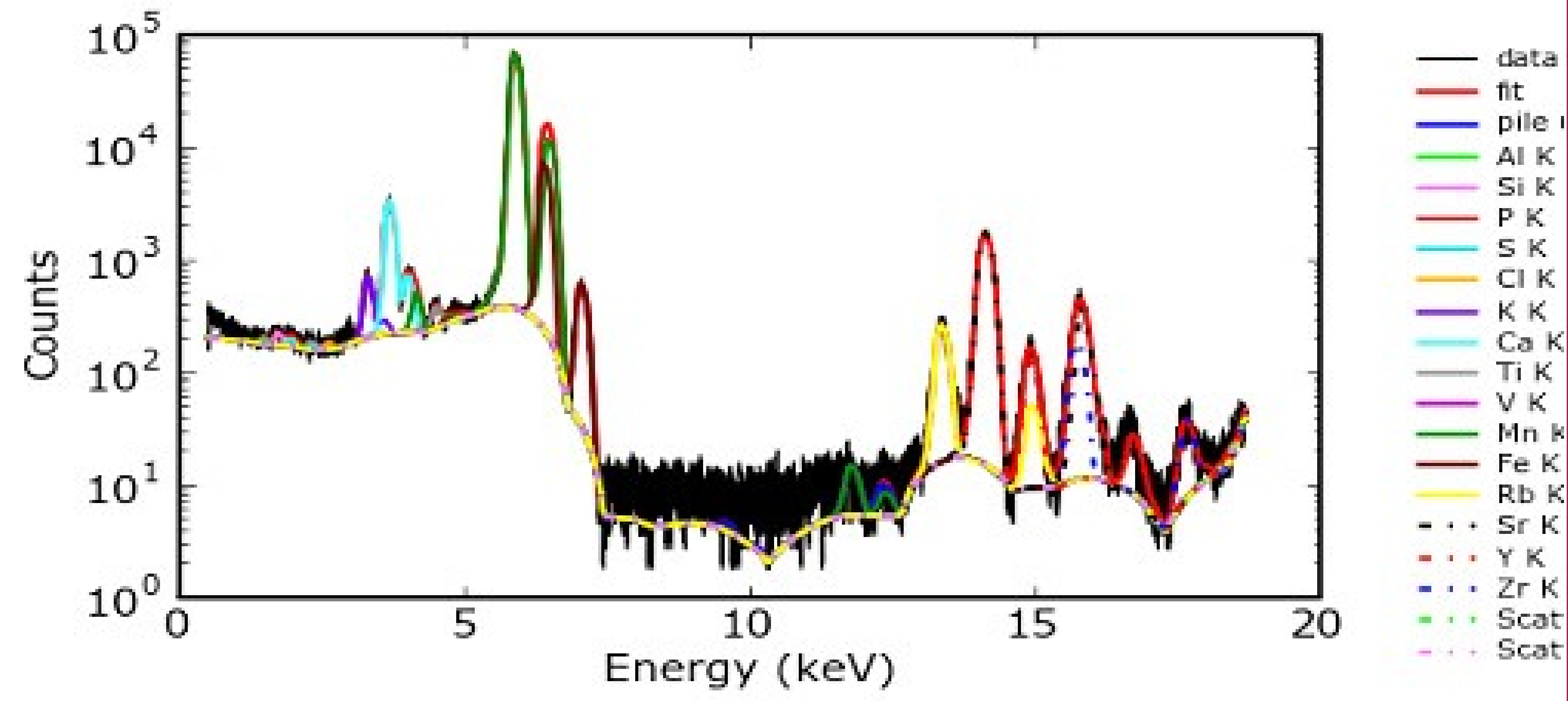

Quantitative data by fitting raw counts with ZAF correction

Often, semi-quantitative data is enough

From Soleil website

X-ray absorption spectrum (XANES)

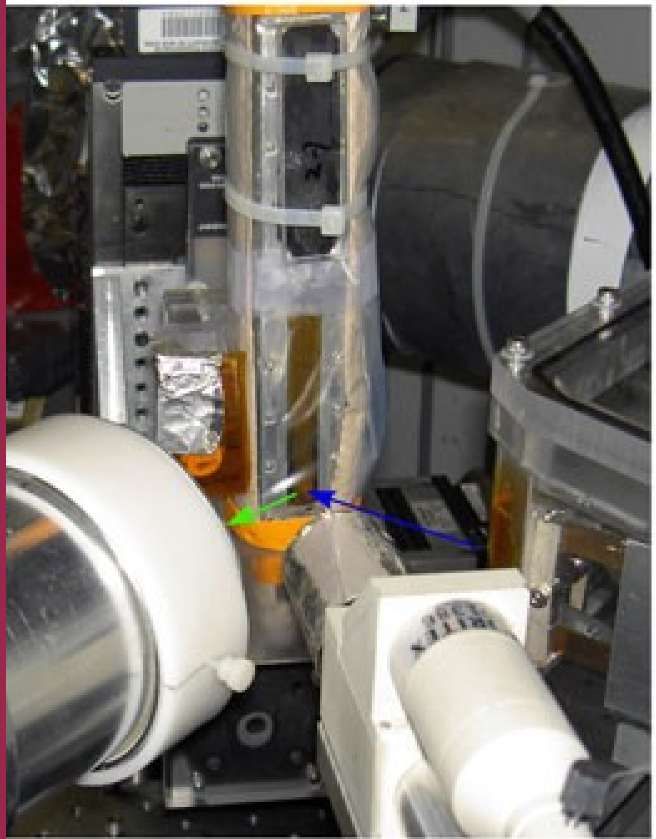

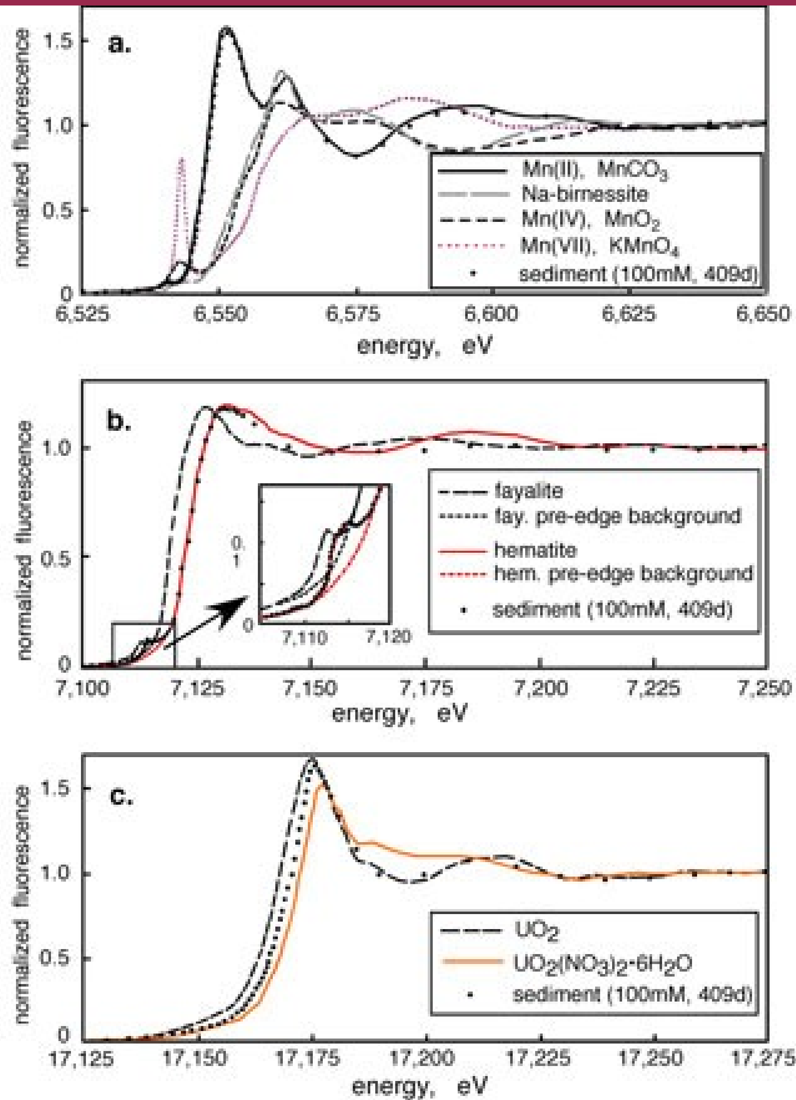

From NSLS website

Microfluorescence science research

Archaeological and cultural heritage

Biomedical

Environmental

Geological

Material science

In situ experimental studies

We will start with some of my geochemistry research because I know it the best . . .

Roots of aquatic plants and sediments

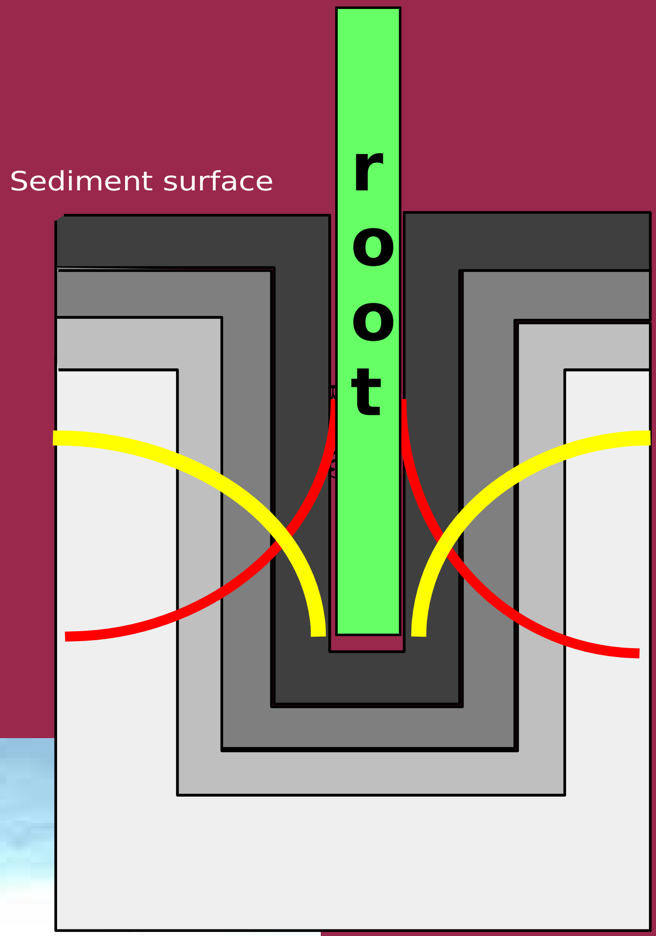

Dissolved oxygen decreases away from root surface

Dissolved iron decreases towards the root surface

Rhizoconcretions formed around roots of *Spartina maritima*

Element	Rhizoconcretion	Sediment
Fe	11.7 %	4.9 %
Cu	60 ppm	29 ppm
Pb	185 ppm	50 ppm
Zn	490 ppm	90 ppm

Significantly enriched in metals compared to sediment How are they distributed?

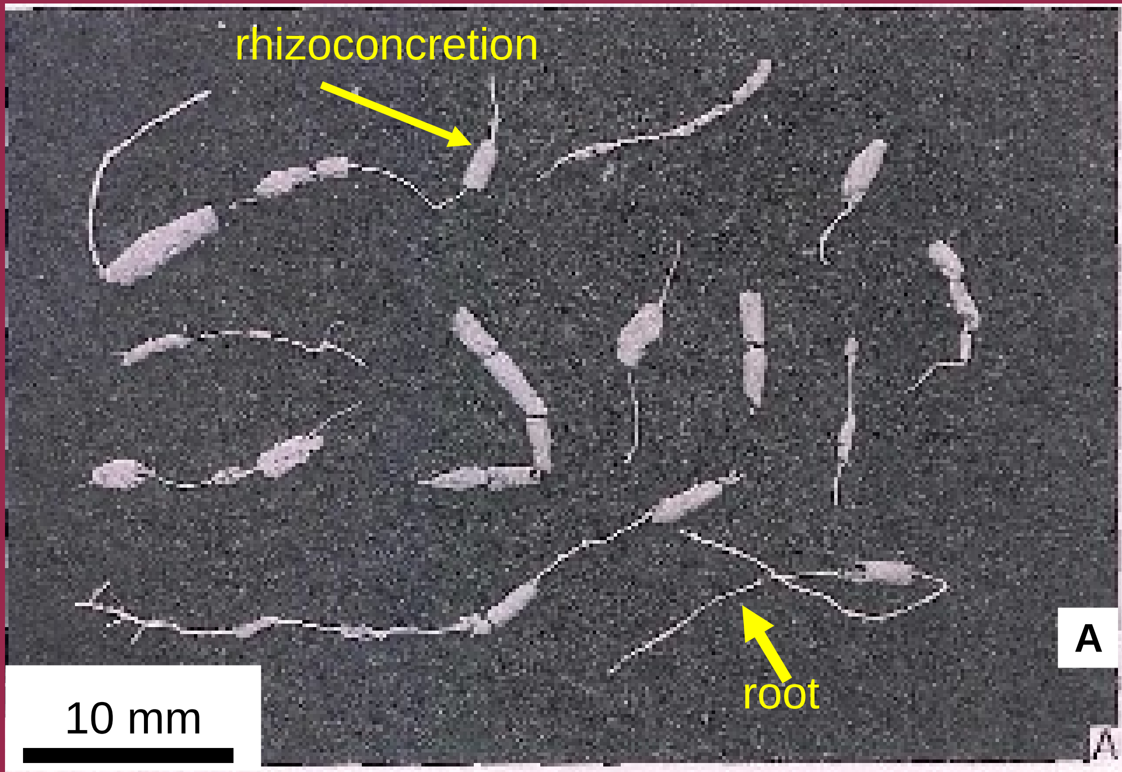

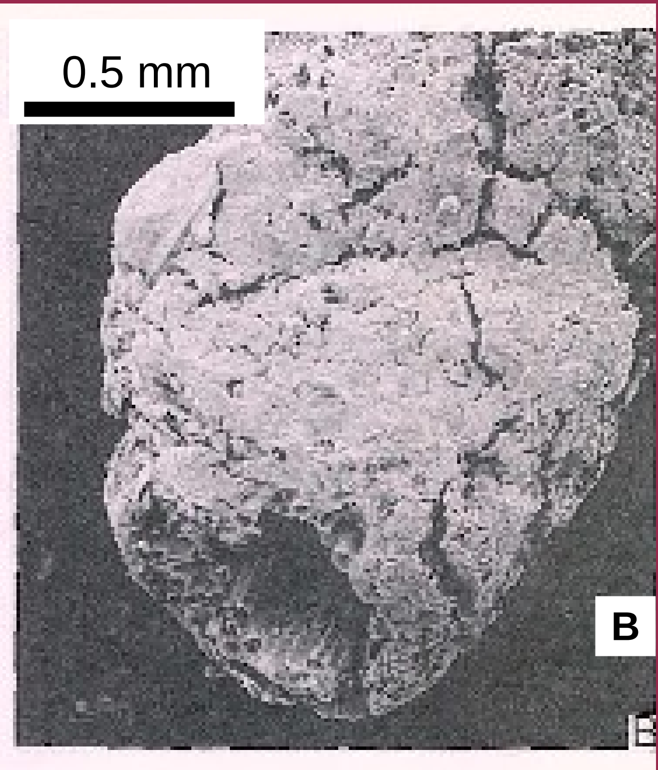

Environmental research

Distribution of metals in rhizoconcretions around S. *maritima*

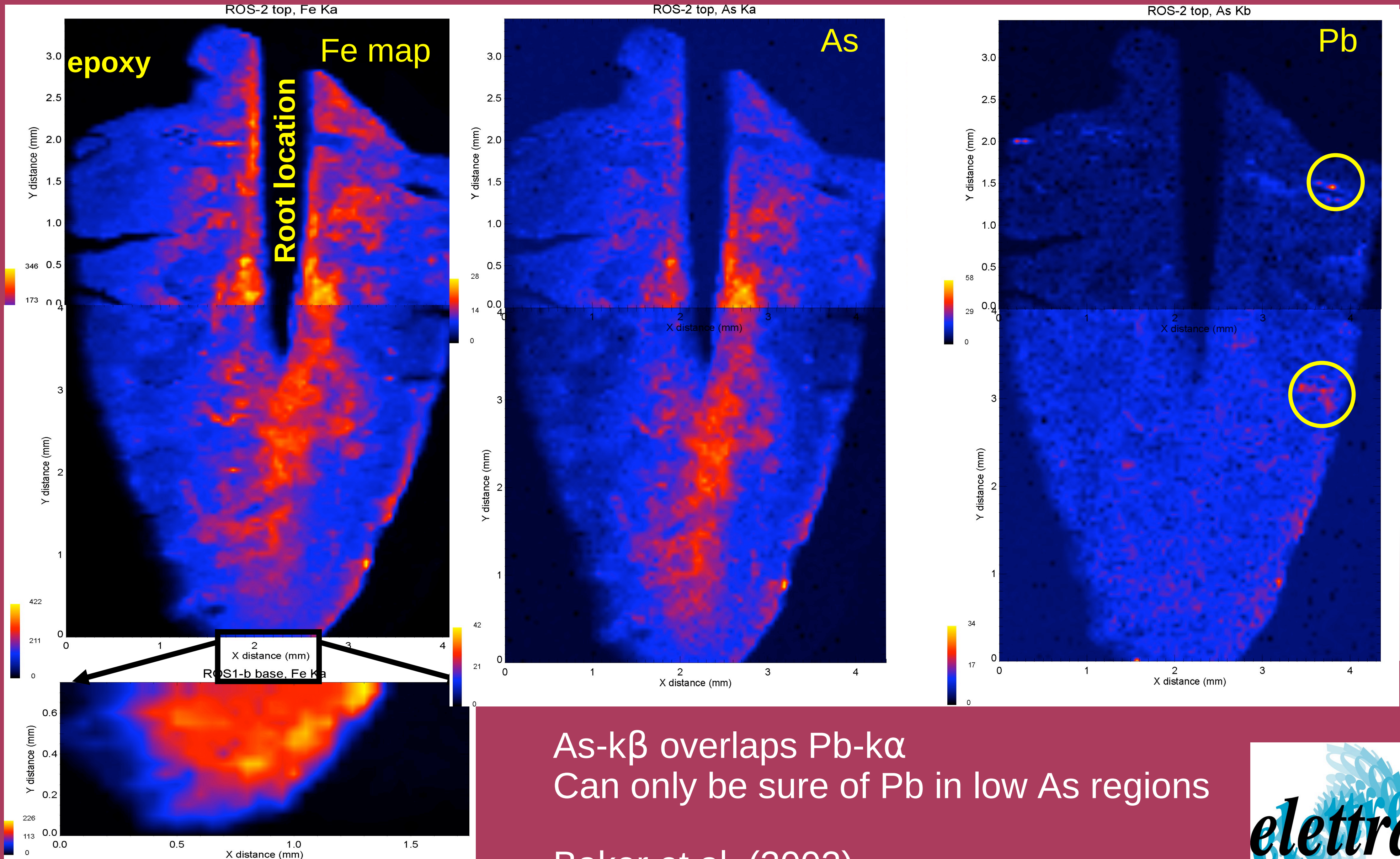

As-kβ overlaps Pb-kα
Can only be sure of Pb in low As regions

Baker et al. (2002)

Geological research

Diffusion and partitioning of trace elements in silicate melts and crystals

Critical for understanding the chemical composition of rocks and the mechanisms that trigger volcanic eruptions and control their explosivity

Continuous eruption, Kilauea, USA

5 April 2003 Stromboli, Italy

Geological research

Diffusion and partitioning of trace elements in silicate melts and crystals

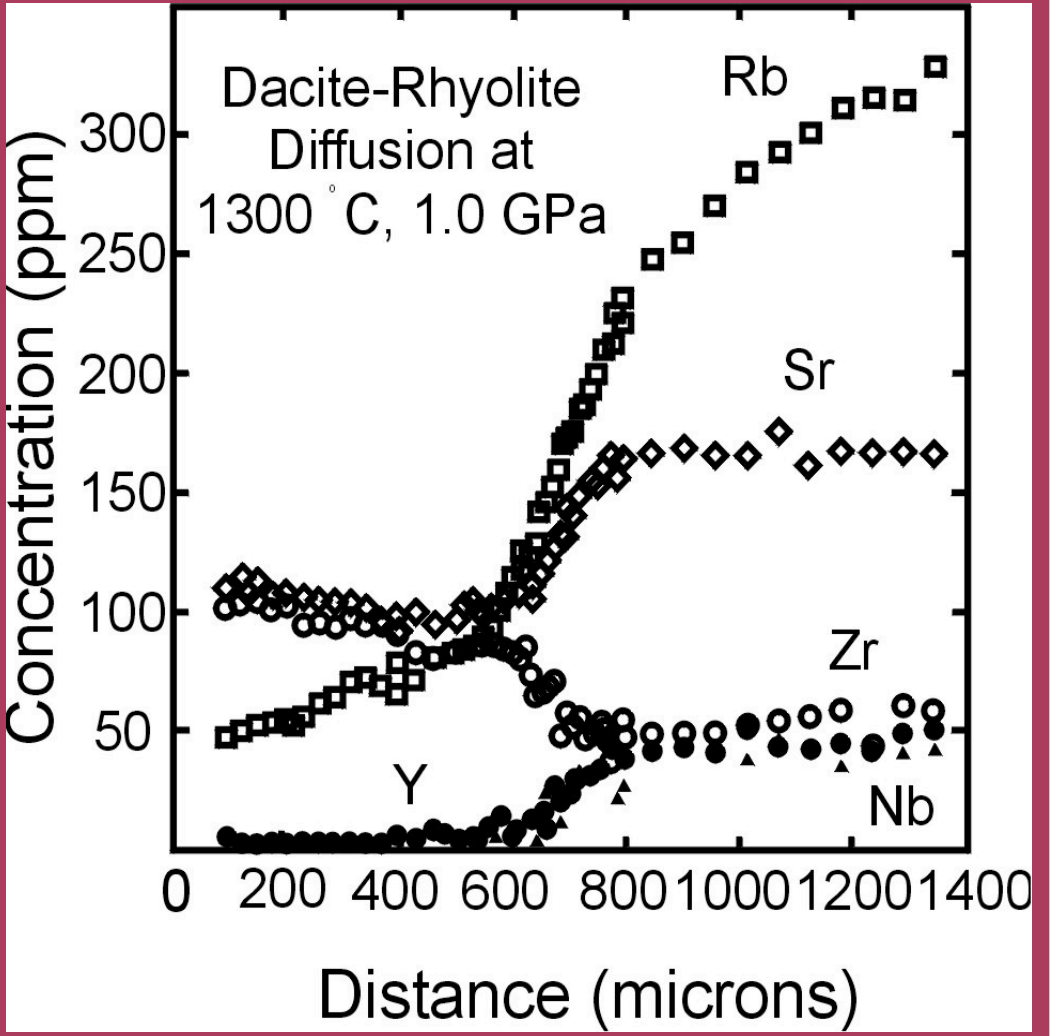

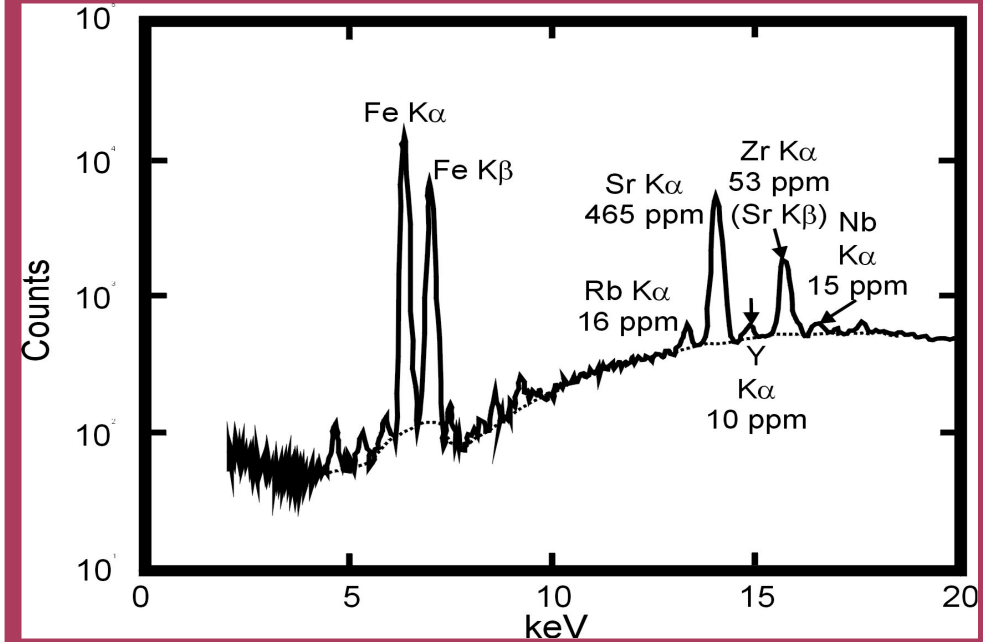

Geological/Materials science research

Micro-XANES allows us to measure the difference between the rates of Fe^{2+} and Fe^{3+} diffusion (Baker et al.)

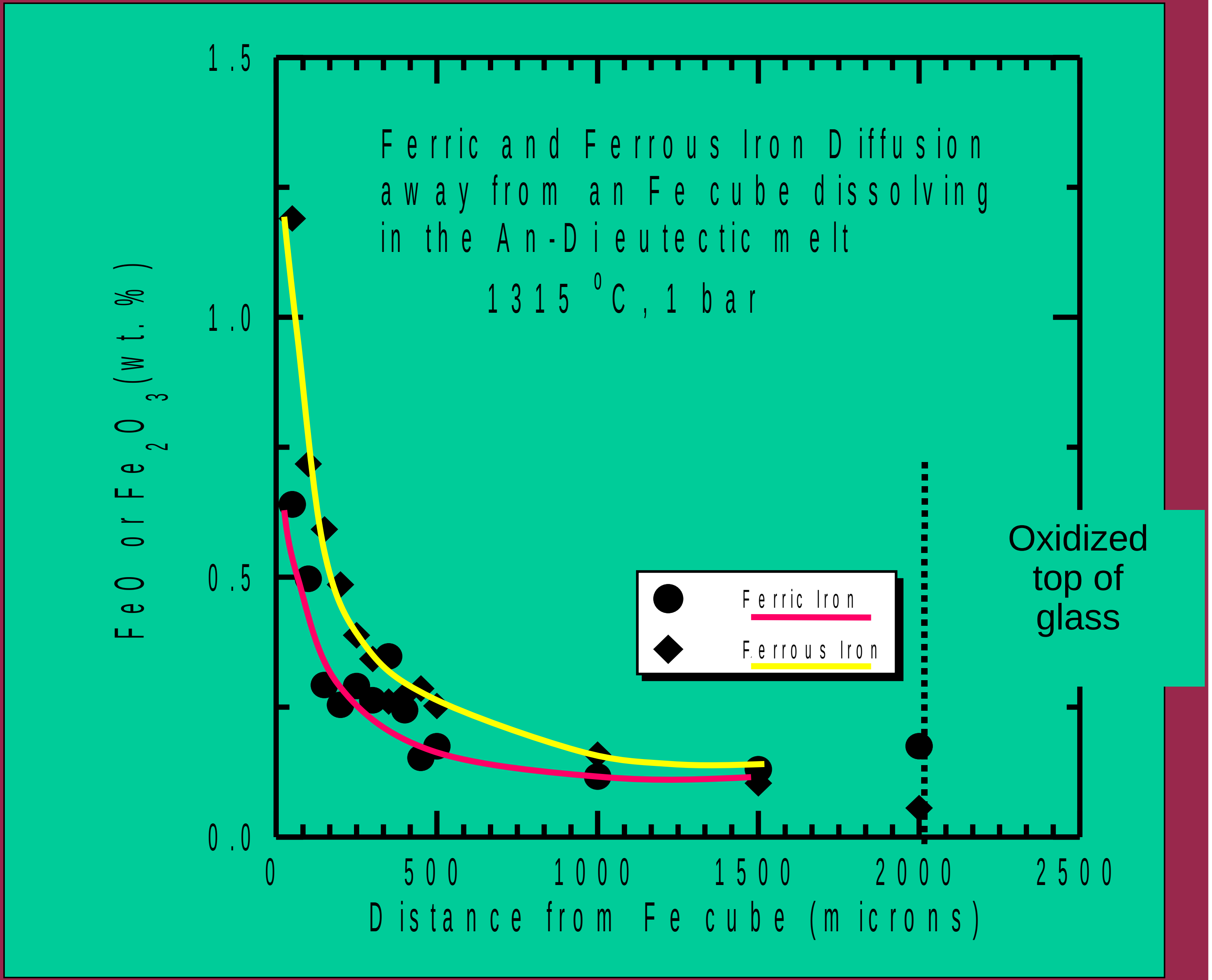

Geological/Materials science research

We still know far to little about the behaviour of sulfur in volcanic systems, even though it has been implicated in global climate change and mass extinctions

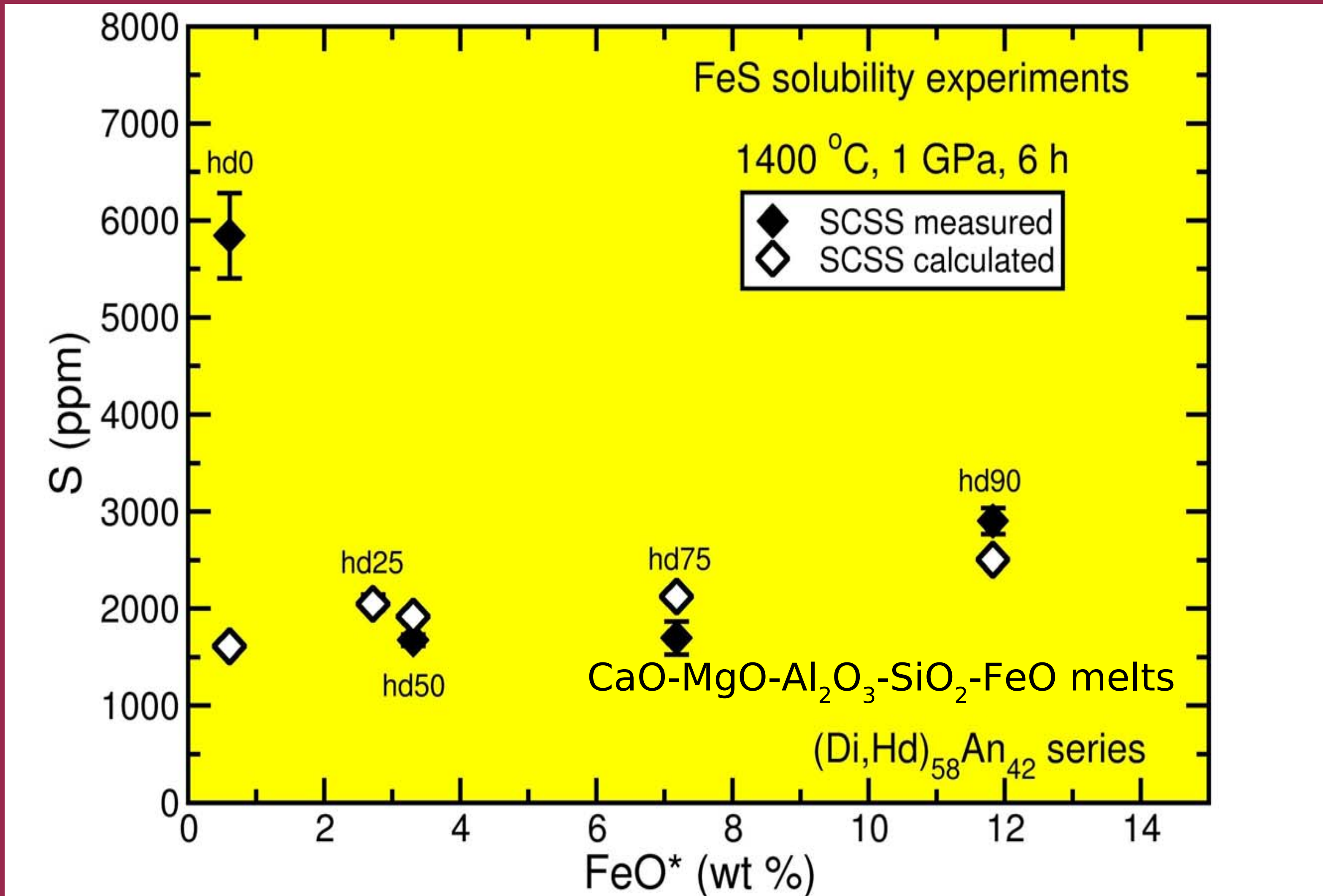

Geological/Materials science research

Sulfur dissolution mechanisms in silicate melts

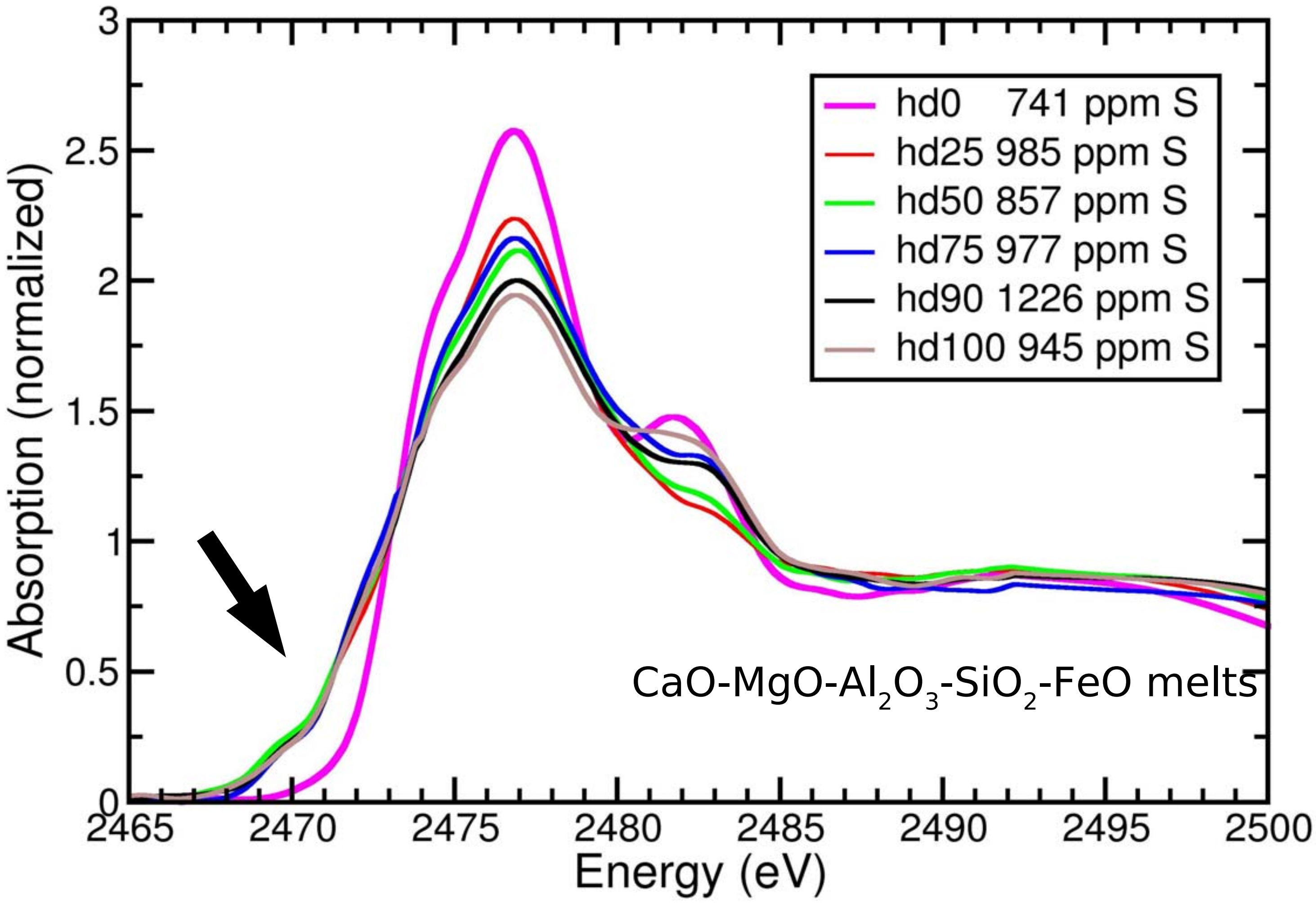

Uniqueness of the hd0 spectrum is the key to its higher SCSS

Geological research

Micro-XANES measurement of Zn coordination in aqueous solutions and in fluid inclusions.

Note "shoulder" in $ZnCl_2$ versus distinct peak in $ZnCl_4$ spectra and position of 2nd-highest peak in $ZnCl_2$ and $ZnCl_4$.

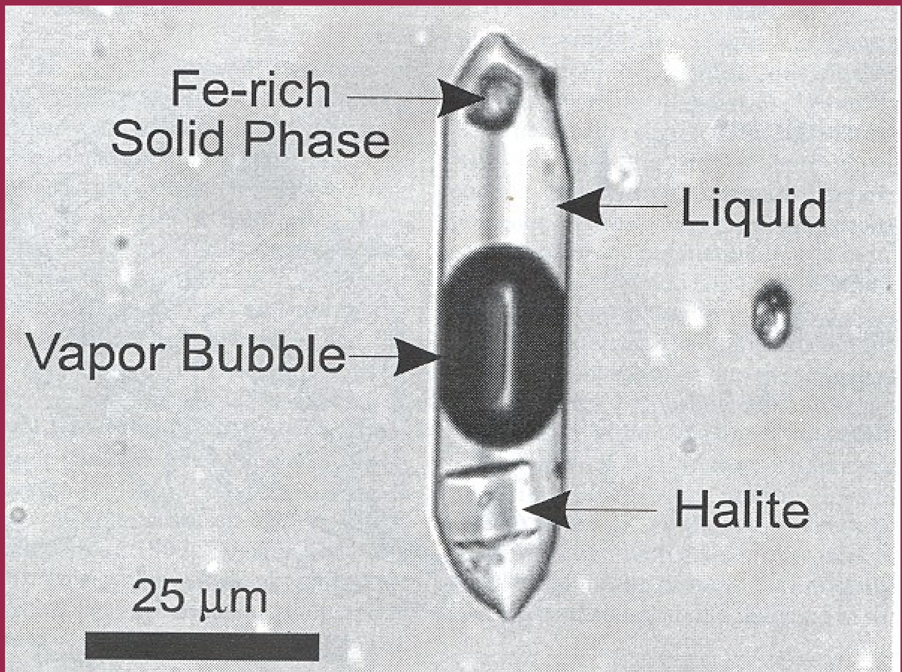

Anderson et al. (1995, 1998)

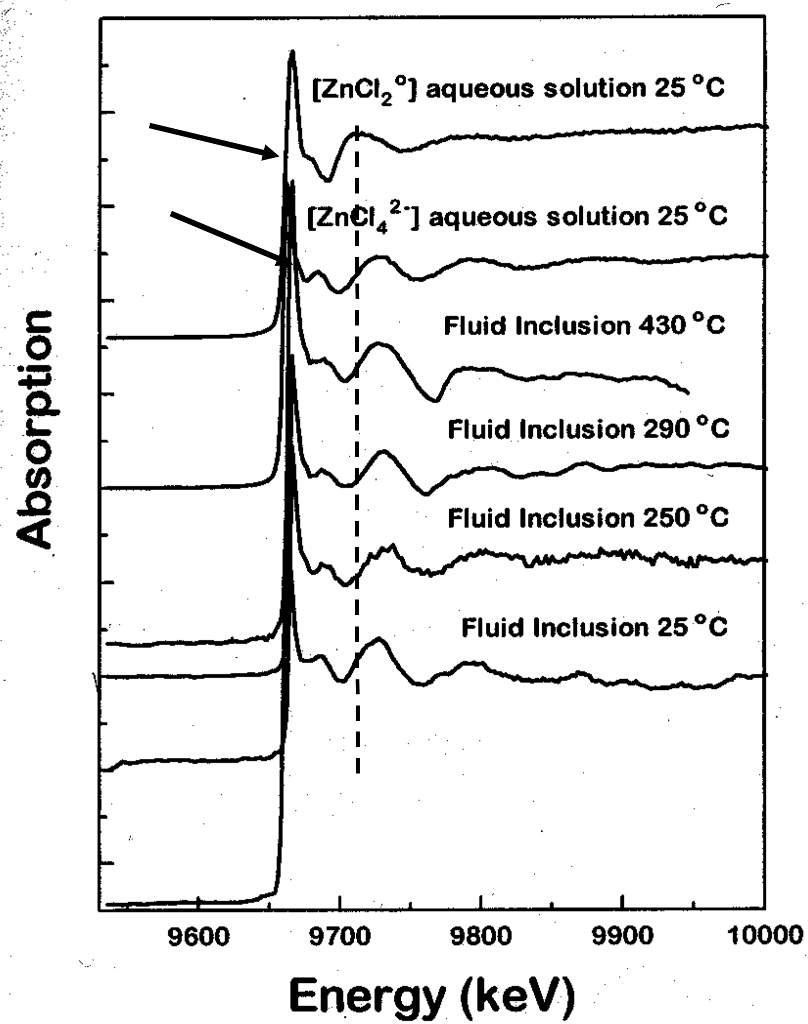

FIG. 5. Zn *K*-edge XAFS spectra collected in the fluorescence mode from a type-1 fluid inclusion at temperatures ranging from 25 to 430°C. Also shown are Zn *K*-edge XAFS spectra collected at room temperature from zinc chloride ($ZnCl_4^{2-}$) and ($ZnCl_2^0$) aqueous solutions.

Geological research

Interplanetary dust particles

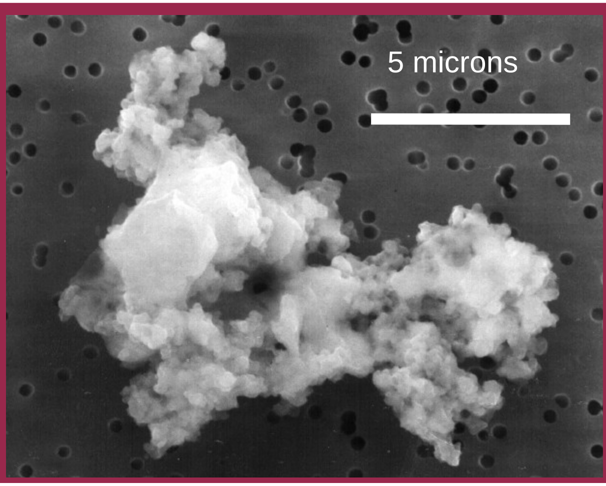

http://antwrp.gsfc.nasa.gov/apod/ap010813.html

Near-chondritic ratios of 1st row transition metals, Ga, Ge & Se

Possibly the most primitive extra-terrestrial samples

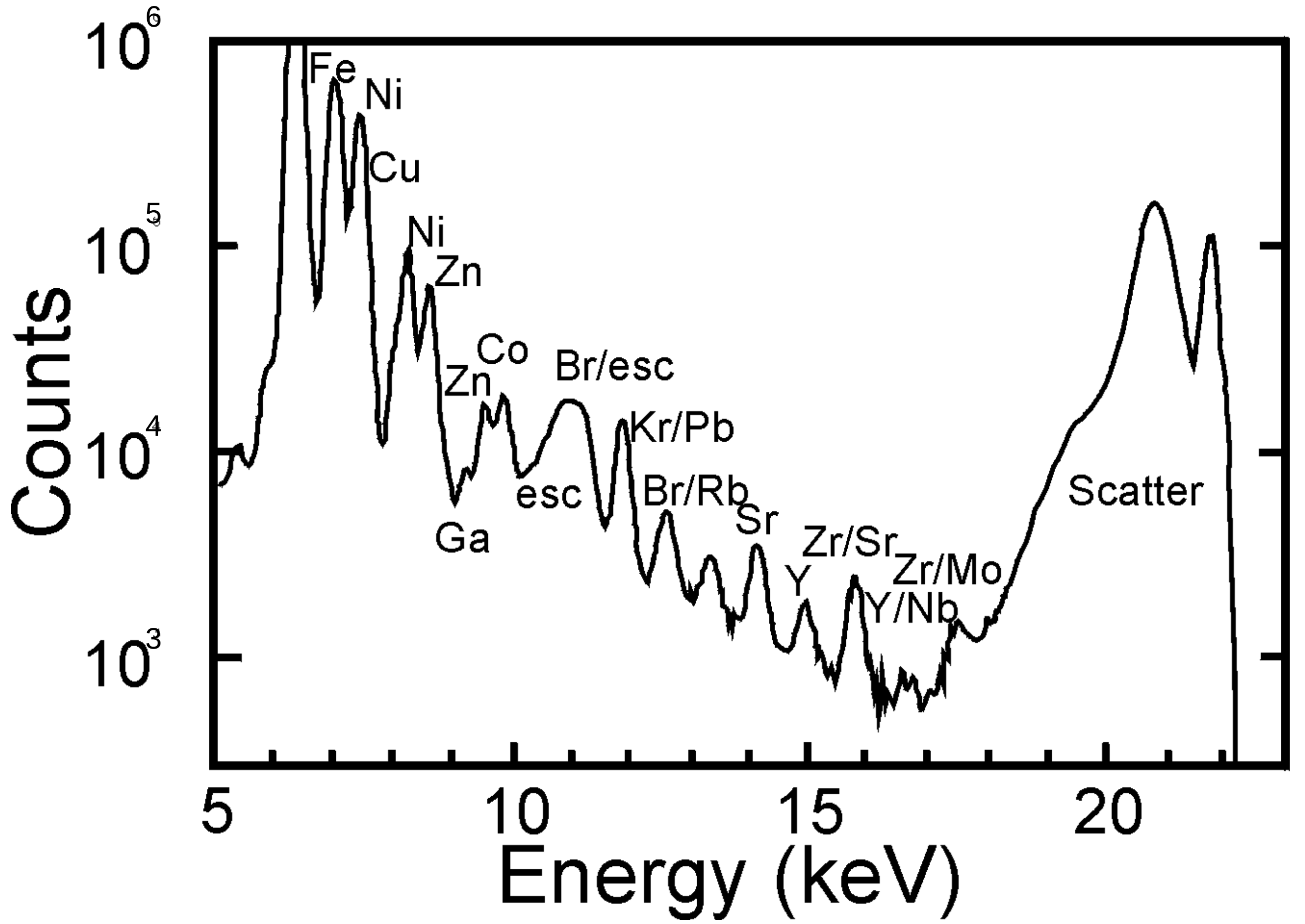

Research by
S. Sutton
GSECARS

In situ experimental studies

Furnaces and aqueous cells can be designed for experiments

For example:

in situ oxidation and reduction at high and low temperatures

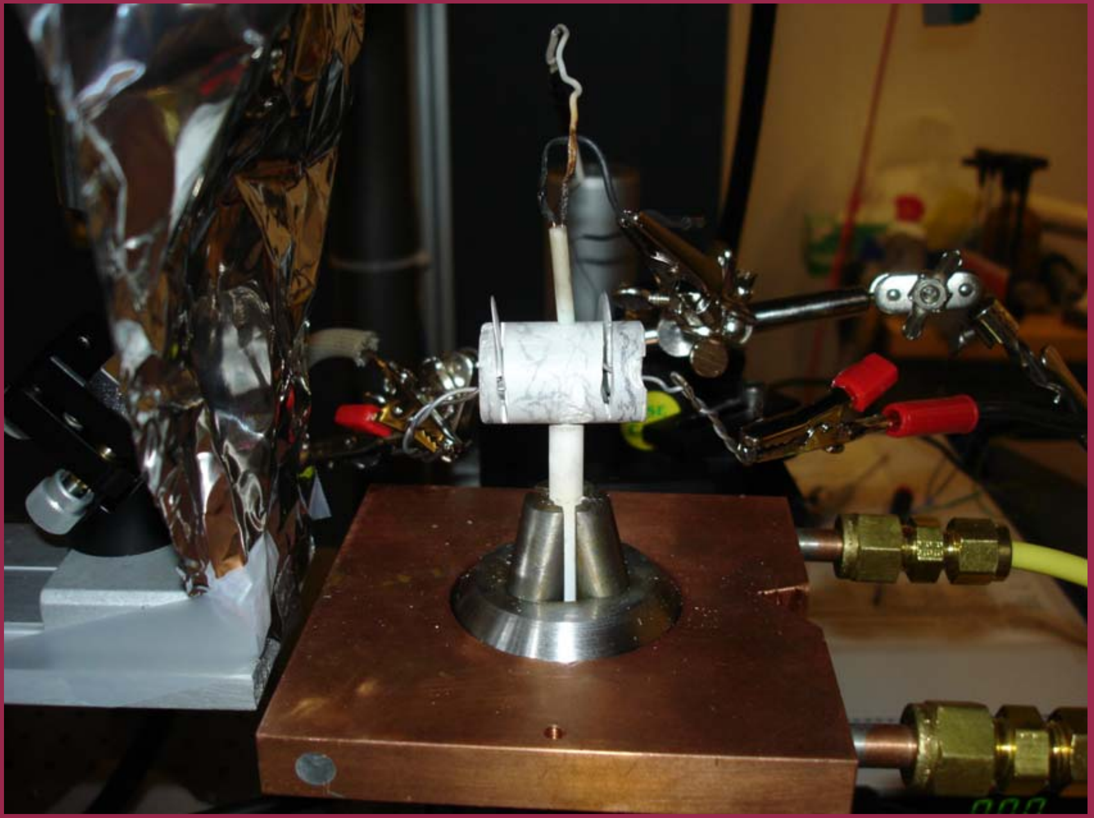

High-temperature furnace for tomography that can be modified for microfluorescence

elettra

Materials science research

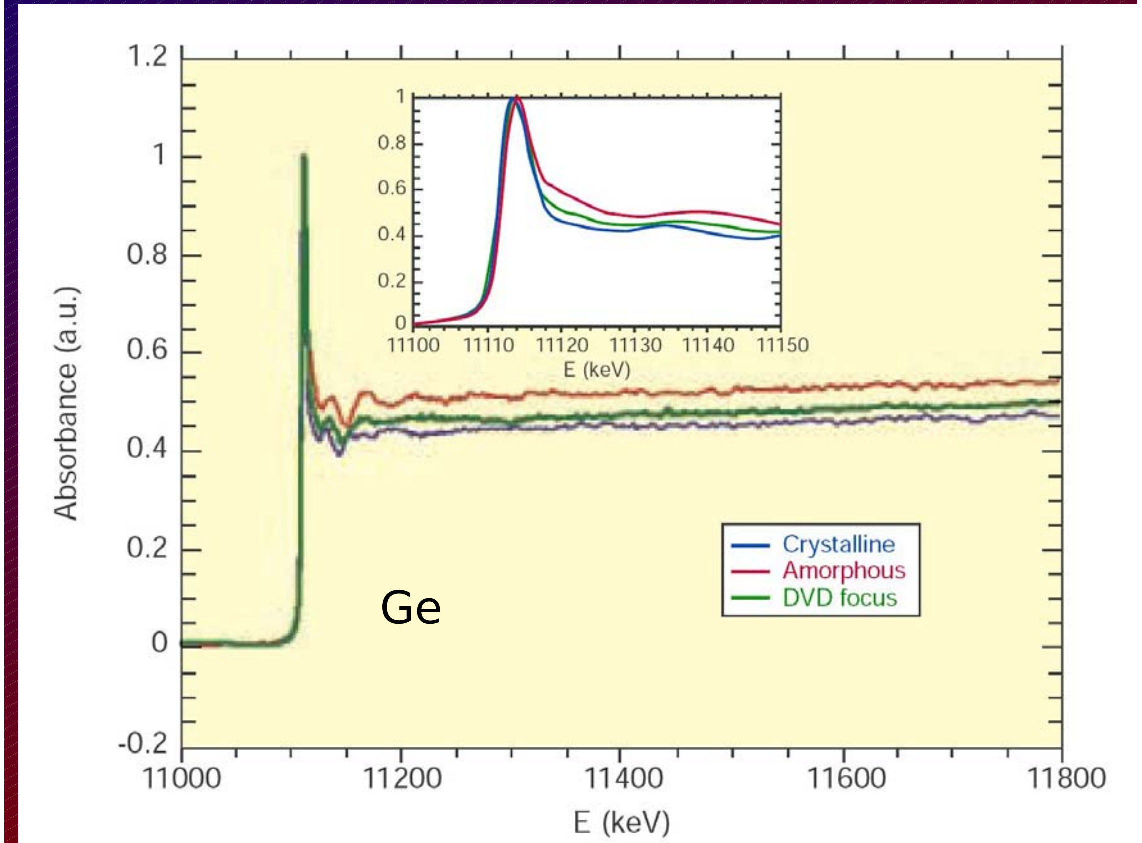

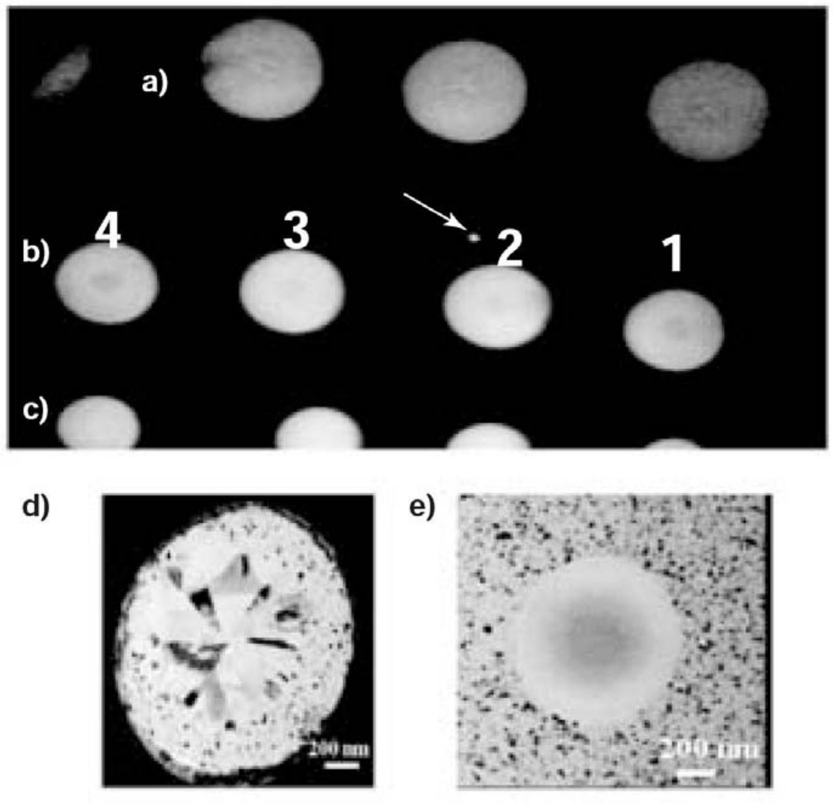

Figure 4

Enlarged DVD spots obtained with laser pulse (λ = 650 nm, 130 mW) of 3 µs (a), 1.5 µs (b) and 800 ns (c). White arrow: 0.5 µm DVD spot. Optical view of (d) crystalline memory point and (e) amorphous memory point. DVD spots numbered from 1 to 4 correspond to numbers in Figure 3.

Structure of DVD memory media

Bohic et al. (2005)

Environmental research

Figure 3

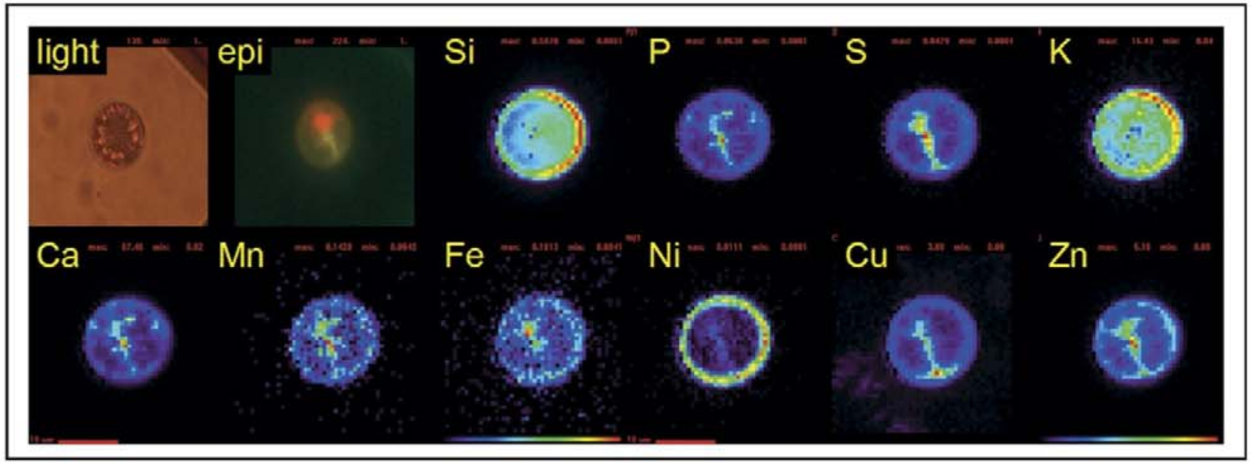

Light and epifluorescence micrographs, and SXRF false-color element maps of a centric diatom collected from the Southern Ocean. Each SXRF image indicates the relative distribution of the specific element and, thus, the concentration scales vary for each image (red scale bars 10 μm). Si and K map onto the frustule of the cell, whereas P, S, Ca, Mn, Fe, Cu and Zn appear to be associated with the cytoplasm of the cell (indicated by the green epifluorescence). Fe is most highly concentrated in the chloroplast (region of red epifluorescence), whereas Zn is colocalized with P (likely to be the cell's nucleus). Ni is found on the outer membranes or frustule of the cell. Figure reproduced with permission from reference [13].

Fahrni (2007)

Environmental research

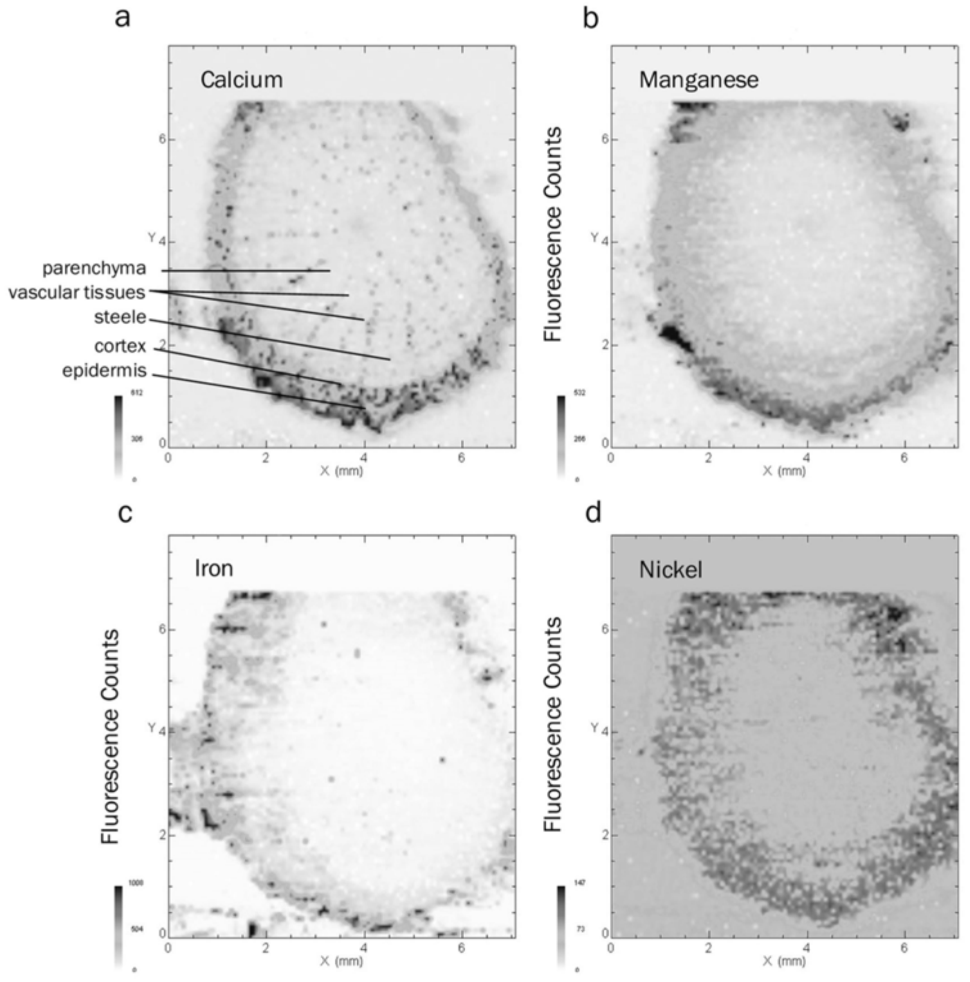

Figure 1. Micro-XRF images of sections (8 mm × 7 mm) of a woody root tissue of *Salix nigra* L. collected from a Ni- and U-contaminated wetland, showing (a) Ca, (b) Mn, (c) Fe, and (d) Ni. Legends indicate raw fluorescence counts.

354 T. Punshon et al.

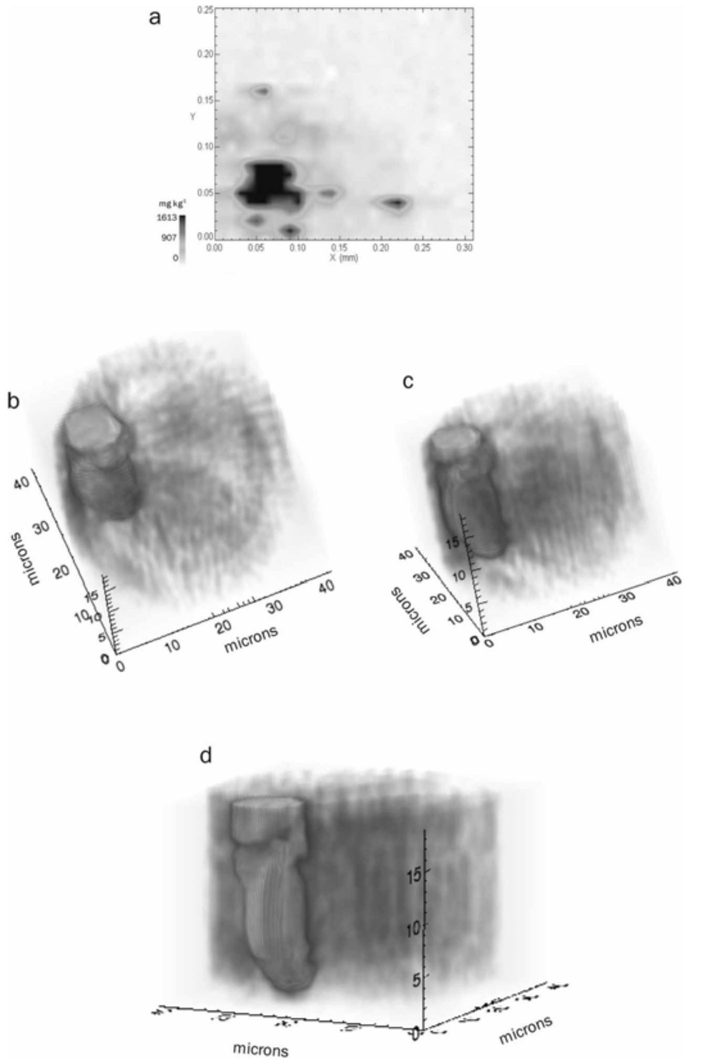

Figure 4. (a) Micro-XRF image (0.31 mm × 0.25 mm) of a Ni-enriched region within the woody tissue of *Salix nigra* L. collected from Steed Pond (from Punshon et al.[19], (b–d) three-dimensional tomographic reconstructions of Ni within the same sample.

Punshon et al. (2005)

Environmental research

Trace elements in tree rings

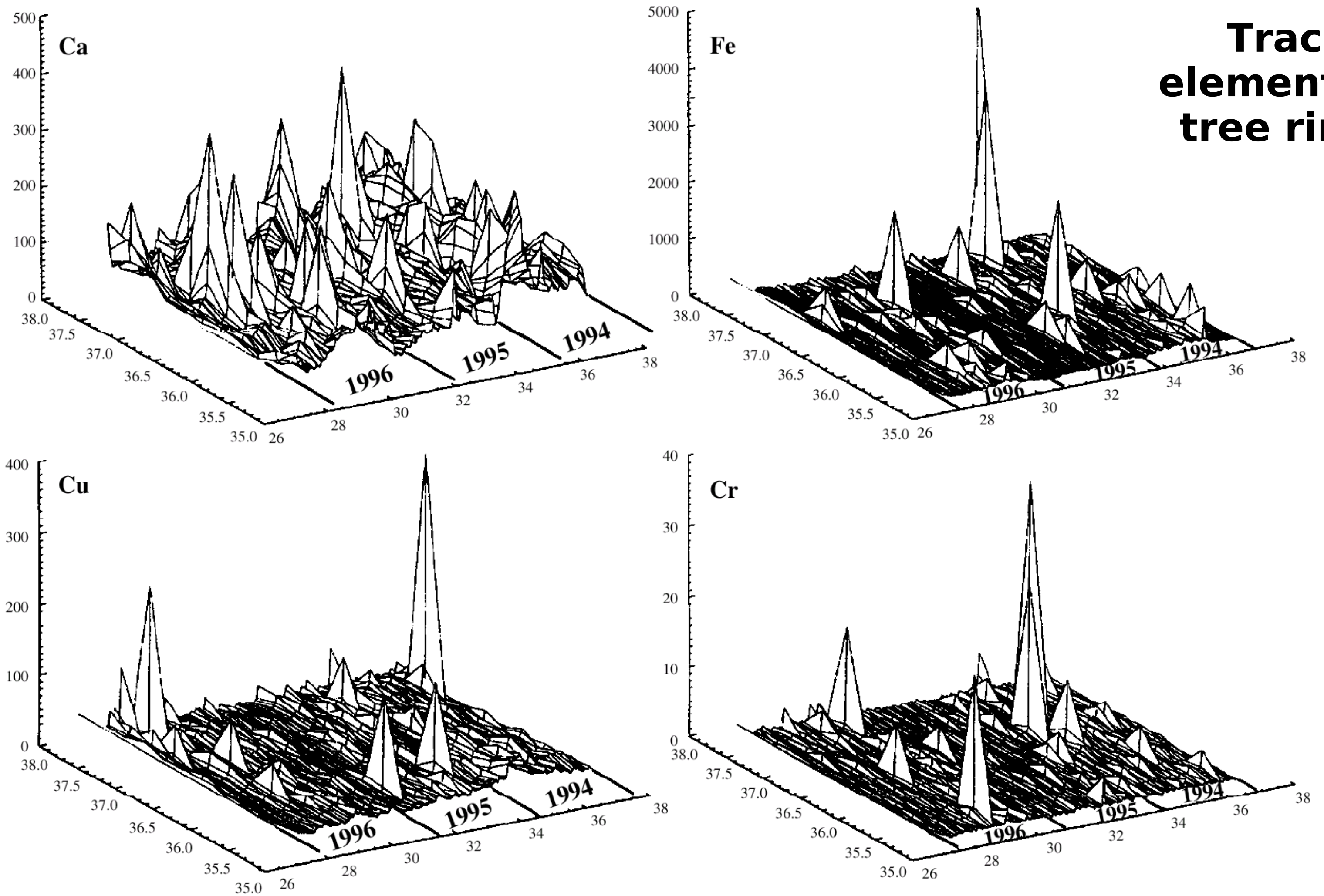

Figure 3. The distribution patterns generated by x-ray fluorescence from Ca, Cu, Fe and Cr. The *x*–*y* plane represents the wood surface, the axes measure the movement of the sample past the x-ray beam (~12 mm in the *x* direction and 2.5 mm in the *y* direction). The x-ray fluorescence intensities, in arbitrary units, for each element are plotted on the *z* axes. The boundaries of the growth rings are shown with the dates corresponding to their year of deposition.

Martin et al. (2001)M

Environmental Research

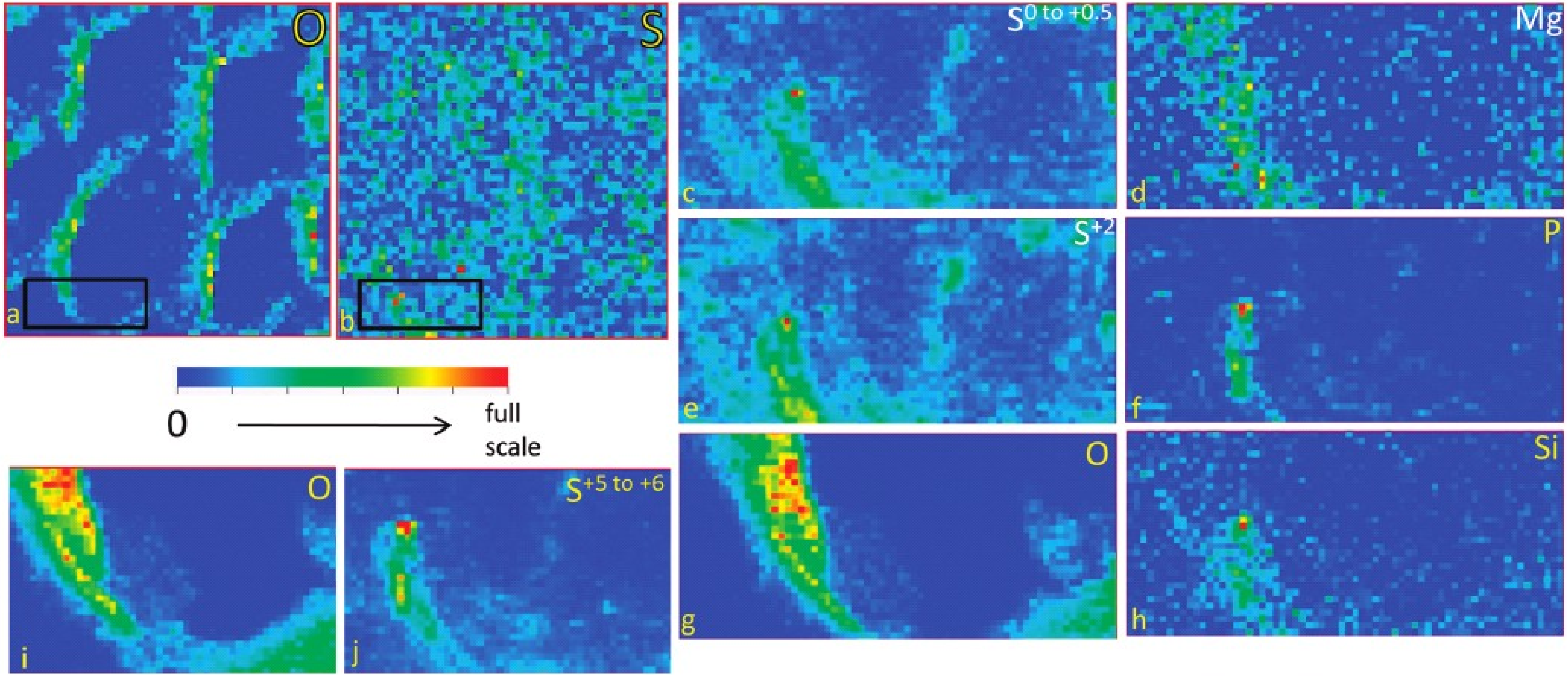

FIGURE 4. Maps of cell walls in the 1985 late wood of sample *Abies* 2. (a) O map and (b) S map of 100 by 100 μm area with 2 μm pixels imaging secondary X-rays. (c−j) Maps of elemental species as labeled using secondary X-ray images (0.5 μm pixels) from the boxed area in b; the area is slightly smaller and displaced in i and j. See Supporting Information for scale quantification.

Fairchild et al. (2009)

Environmental Research

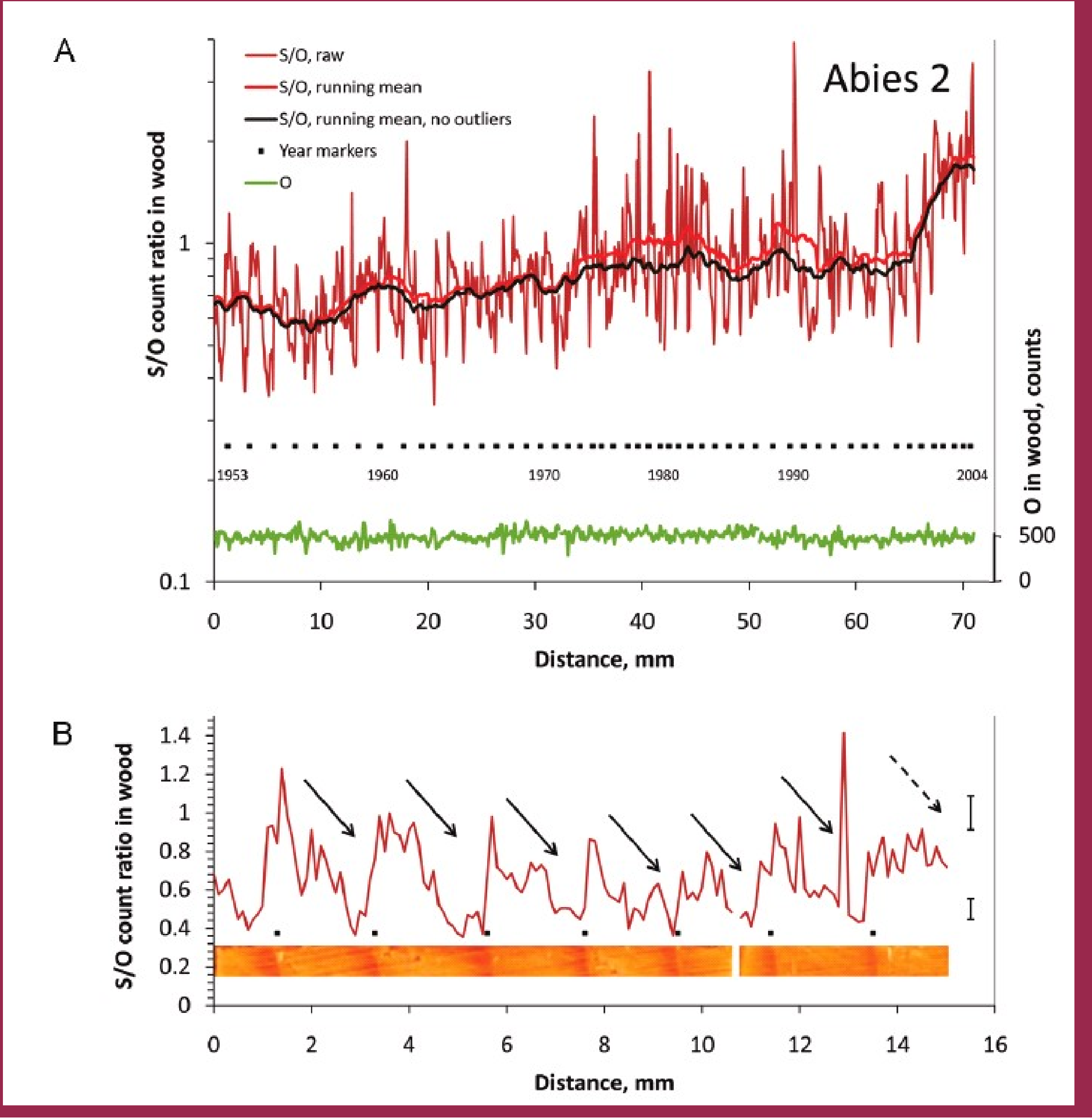

Fairchild et al. (2009)
Note falling S/O ratio
during growth season

Environmental Research

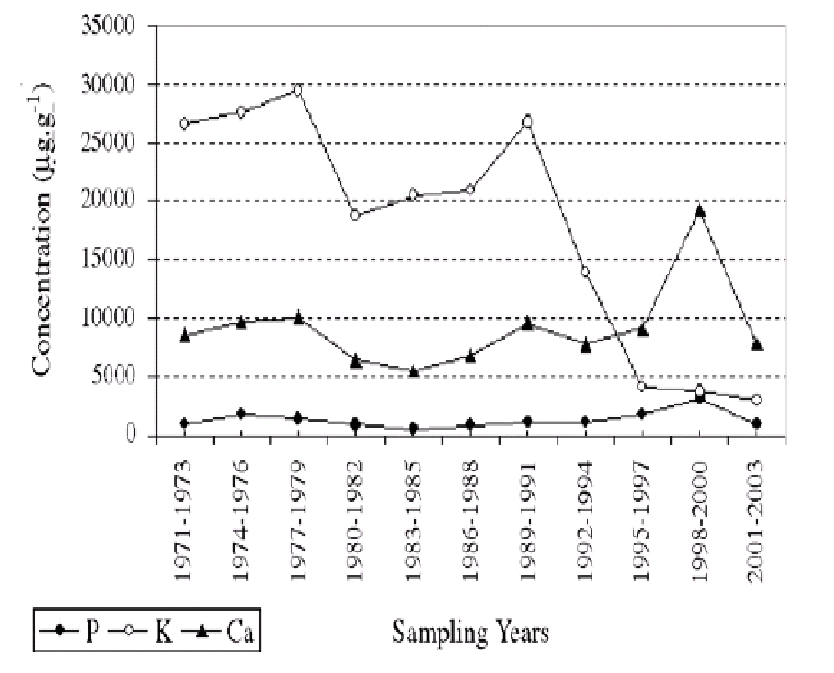

Fig. 3. P, K and Ca distributions in function of sampling years for *Caesalpinia peltophoroide* measured by SR-TXRF.

de Vives et al. (2006)

Leaded gas outlawed in Brazil in 2009

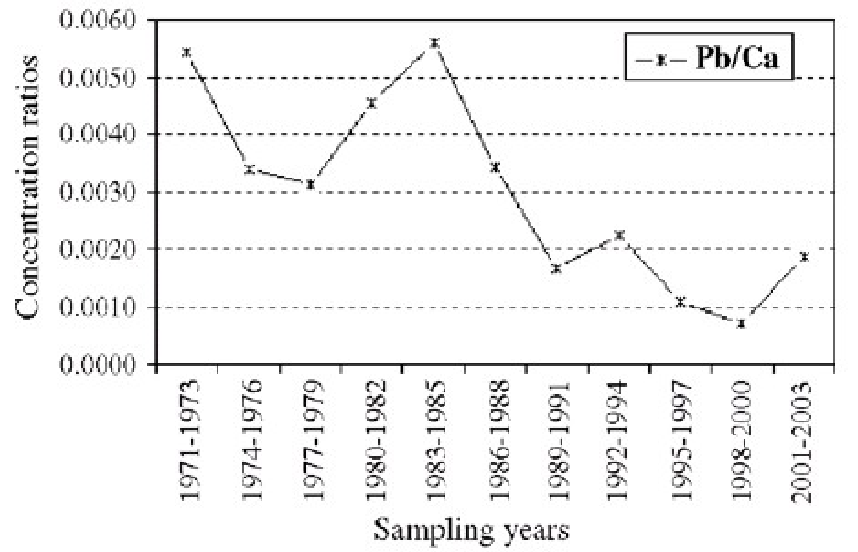

Fig. 6. Pb/Ca concentration ratio in *Caesalpinia peltophoroide* measured by SR-TXRF.

Environmental Research

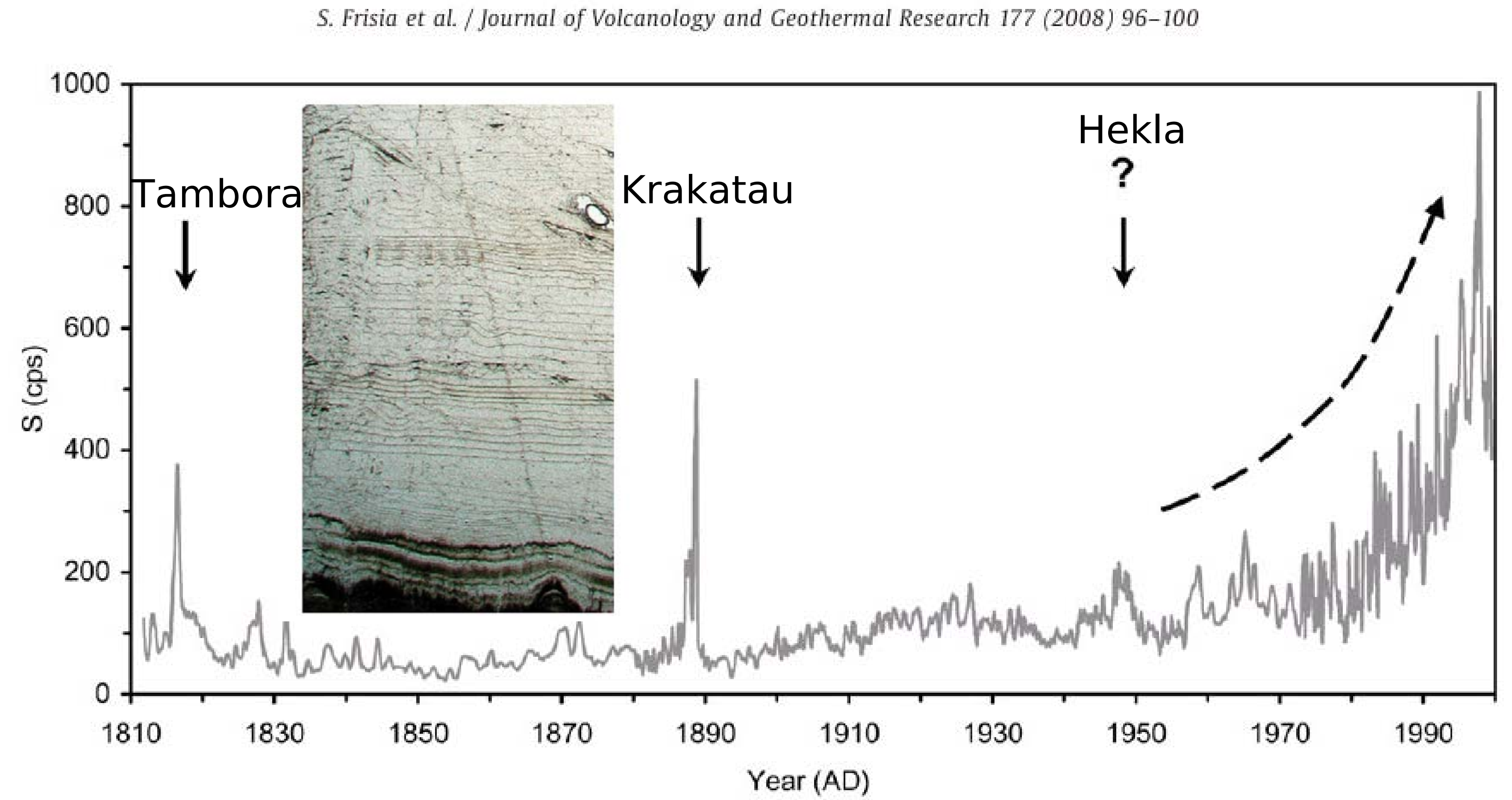

Speleothems and sulfur in the atmosphere

Frisia et al. 2008

Environmental Research

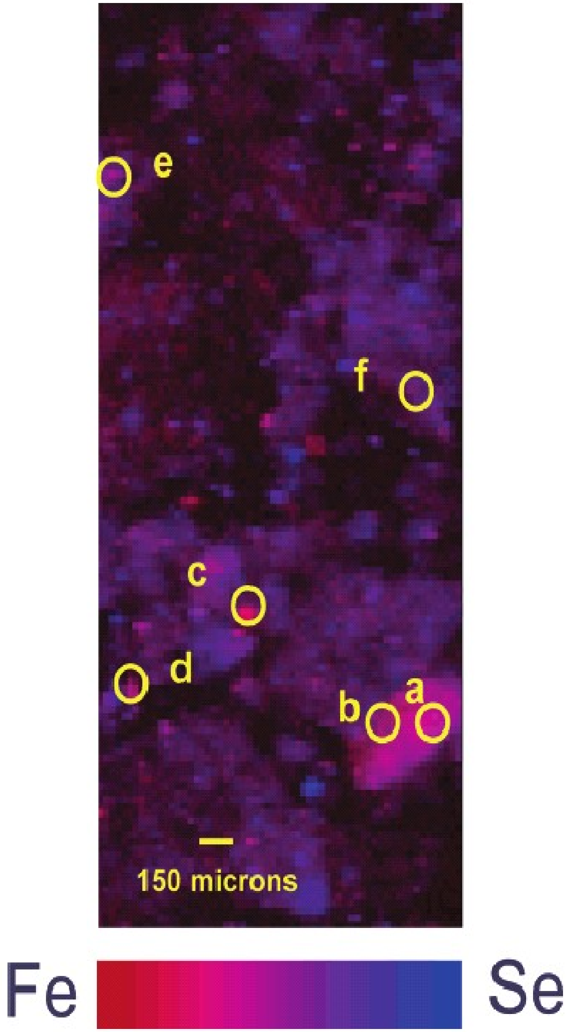

FIGURE 2. Bicolor μ-SXRF map of the reclaimed mine soil sample S3. The letters next to the circles indicate points of interest (POI). The color bar indicates the degree of codistribution of the two elements. Where the elements are not colocated the color is either pure red (Fe) or pure blue (Se); when the elements are both located at a pixel spot red and blue are mixed resulting in the colors indicated in the color mixing bar.

Se in reclaimed mine site

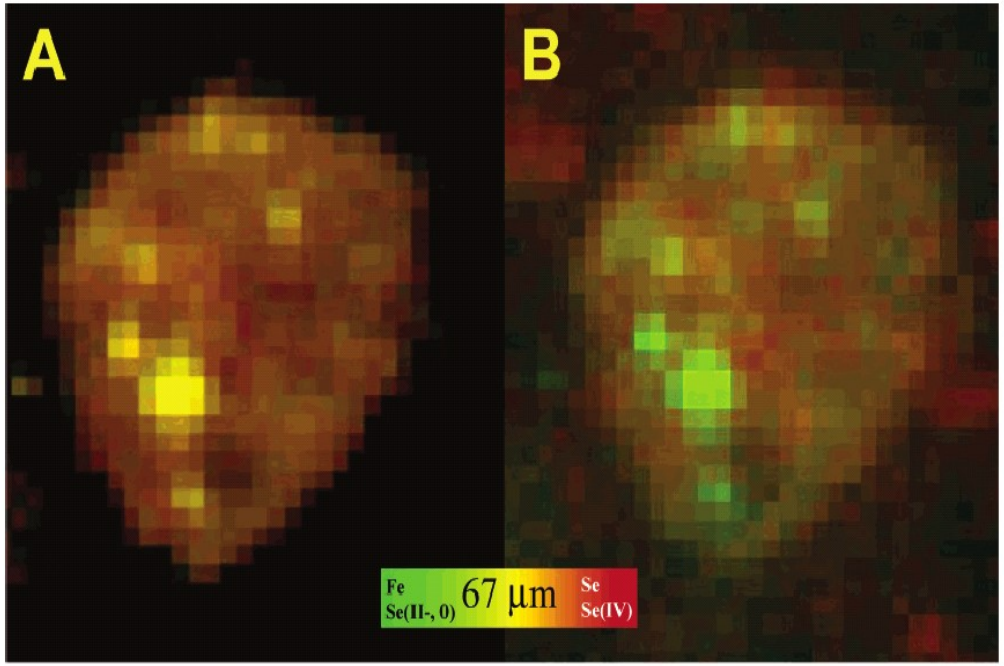

FIGURE 5. Bicolor micrographs for Se oxidation states (panel A) and Se and Fe distribution (panel B). The color bar indicates relative mixing of oxidation states and Fe and Se. Micrograph A is an oxidation state map created by mapping at 12658.8 eV where the Se(0)/Se(IV) was maximized (green), followed by another scan at 12664.5 eV where Se(IV)/Se(0) was maximized (red). The resulting micrograph indicates the relative spatial distributions of Se(−II, 0) and Se(IV). Micrograph B is a bicolor map for total Se (green) and iron (red) scanned at 12683.0 eV. Brightness, saturation, and contrast were modified to enhance spatial distribution information.

Ryser et al.
(2006)

Environmental research

Investigations of contaminated soils

Steve Sutton
GSECARS, APS

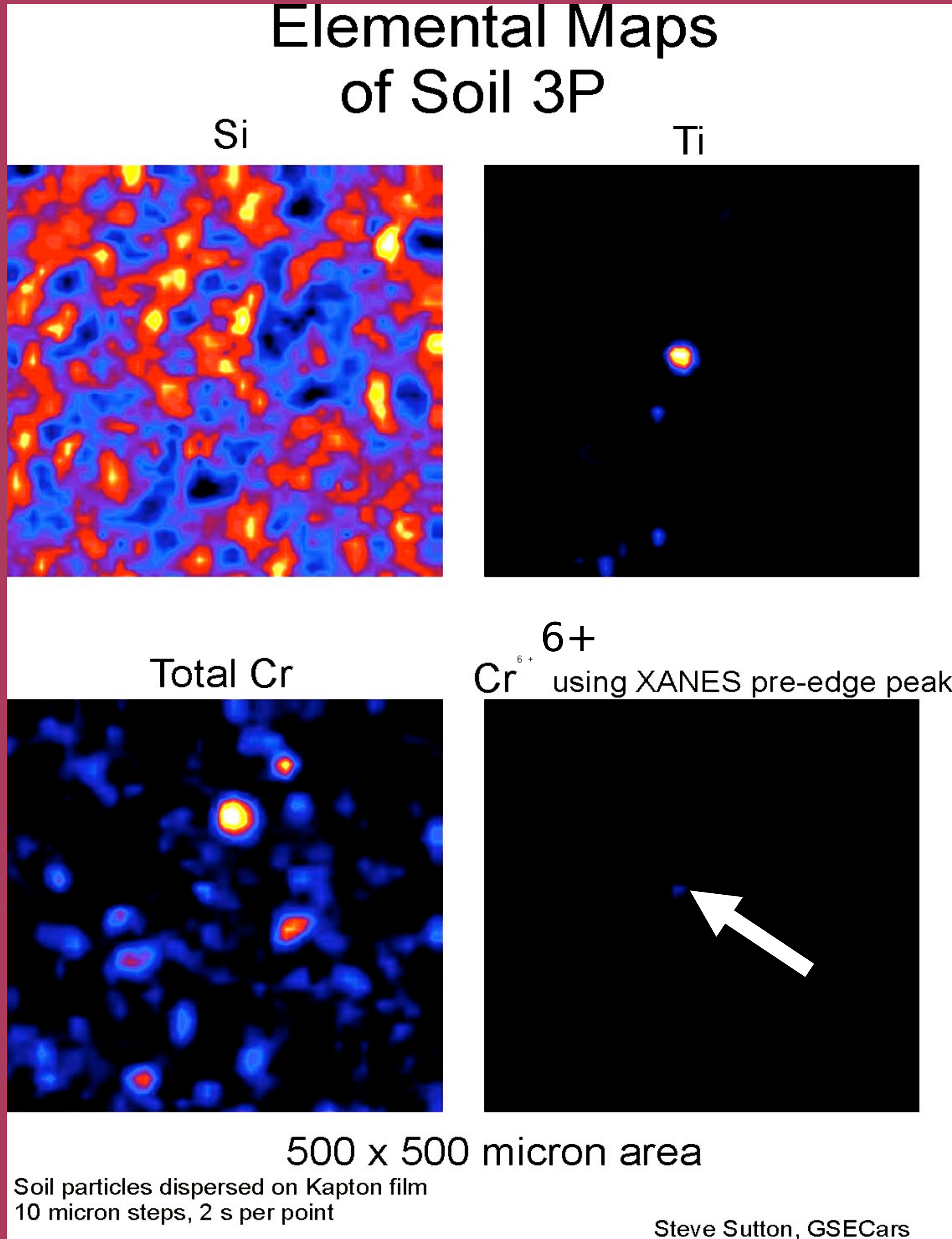

Environmental research

Samber et al. (2008)

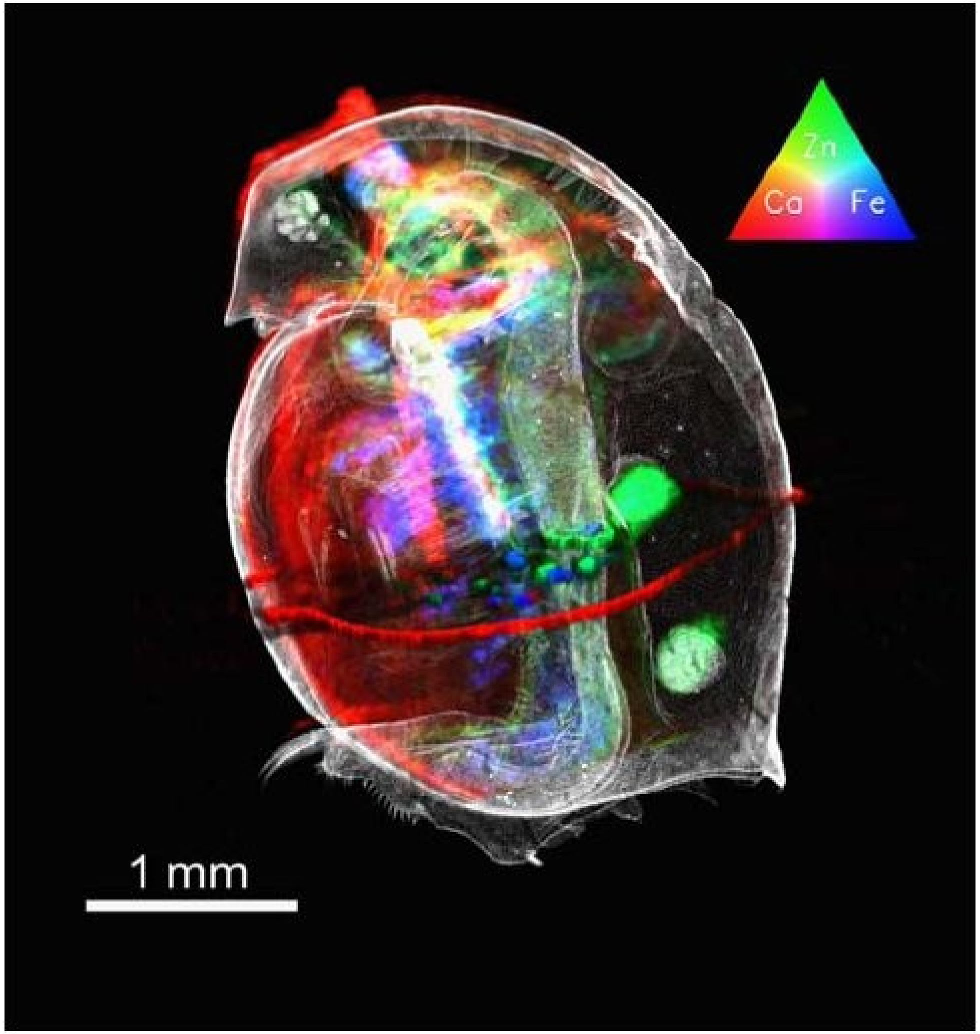

Fig. 3 Three-dimensional rendering of the unexposed *Daphnia magna* sample shown in Fig. 2 (*left side*). The grayscale dataset gives a full 3D absorption reconstruction of the daphnid (3-μm resolution) obtained by the UGCT micro/nano CT setup at Ghent University. Two RGB composed micro-XRF datasets obtained at HASYLAB, Beamline L are also incorporated in the image: a micro-XRF 2D dynamic scan (height 175×20 μm, width:122×20 μm) and a micro-XRF computed tomography cross section (width 165×20 μm) through the gill tissue, eggs, and gut

Biomedical Research

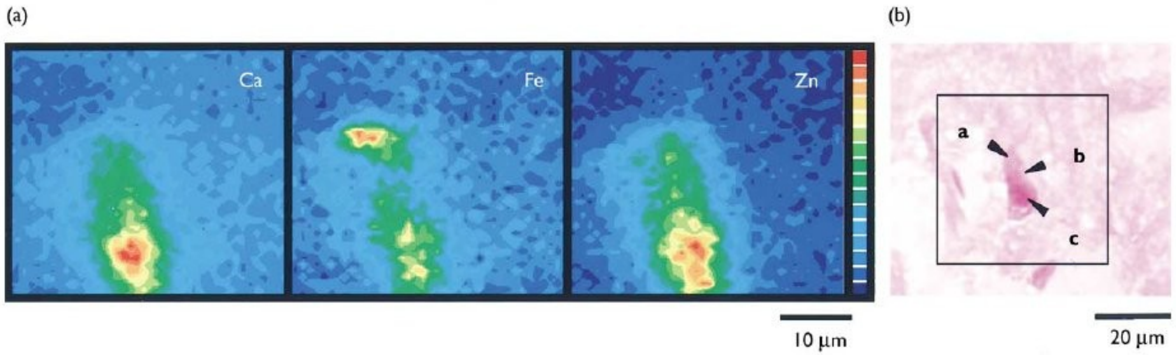

Fig. 1. (**a**) X-ray intensity maps (Ca, Fe and Zn) of a neuron in the scanned area of the tissue section from an AD brain. The scanning area was 40 × 40 µm and divided into 40 × 40 pixels of 1 µm. Each measurement point of the sample was irradiated for 5 s. The scale on the right shows the counts of the X-ray intensity. The range of mapping was 20–280 for Ca, 0–90 for Fe, and 0–120 for Zn. (**b**) Micrograph of the scanned area of the frozen brain tissue section stained with HE. The neuron corresponds with the images of (**a**). (**a**–**c**) show the measurement points.

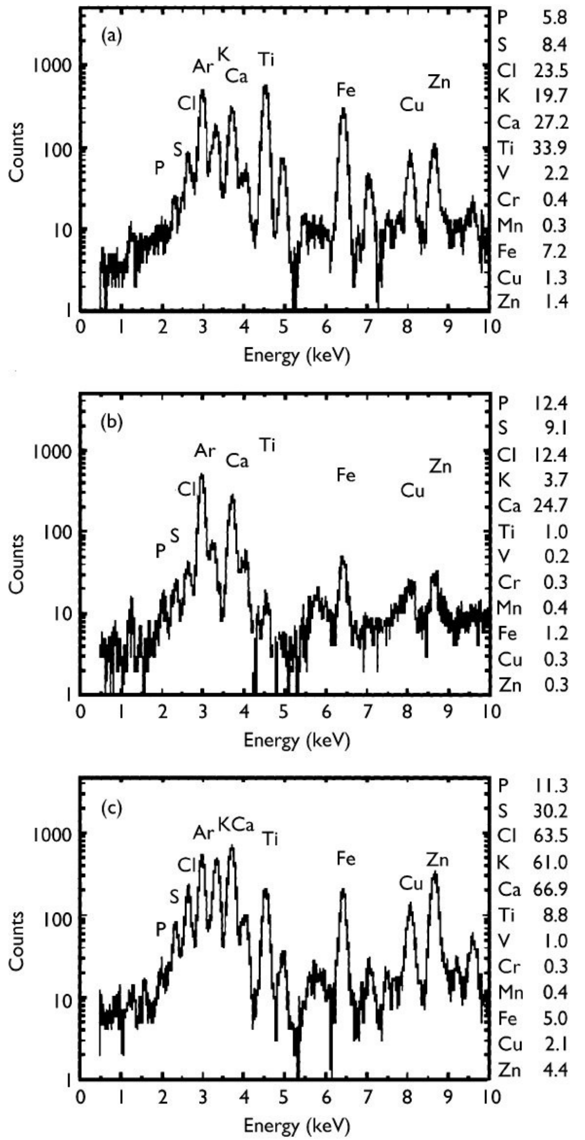

Fig. 2. Fluorescence X-ray spectra inside the neuron shown in Fig. 1b. The measurement points were (**a**) and (**b**) cytoplasm and (**c**) nucleus. The X-ray energy was 14.9 keV. Ratios of the elemental concentrations to Ar at the measurement points are shown at the right side of the graphs.

Alzheimer's Disease
Ishihara et al. (2002)

Archaeological and cultural heritage

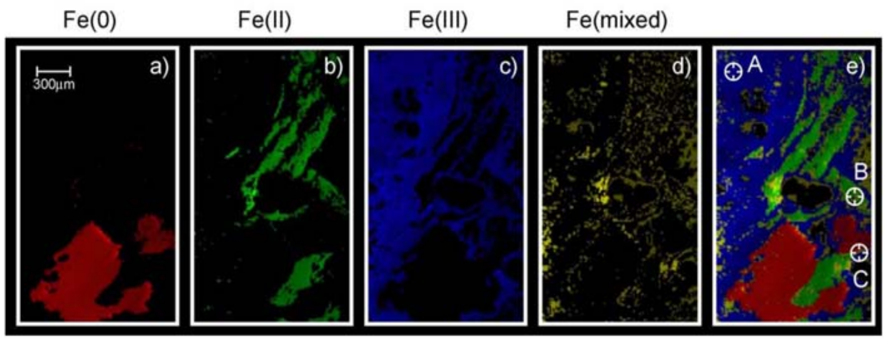

Fig. 8. Distribution of iron oxidation states within a selected area of a Roman smithing waste sample. Oxidation state maps representing areas with predominant occurrence of (a) Fe^0, (b), Fe^{II}, (c) Fe^{III}, and (d) areas with multiple iron oxidation states present. (e) Complete oxidation state map. Markers and labels indicate locations selected for micro-XANES and micro-EXAFS investigations (Fig. 9).

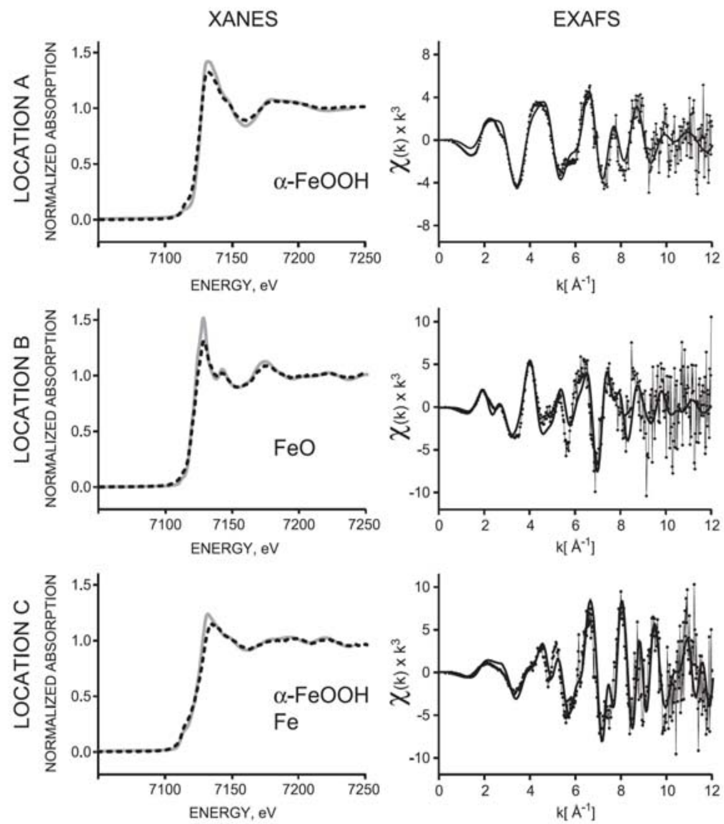

Grolimund et al. (2004)

Archaeological and cultural heritage

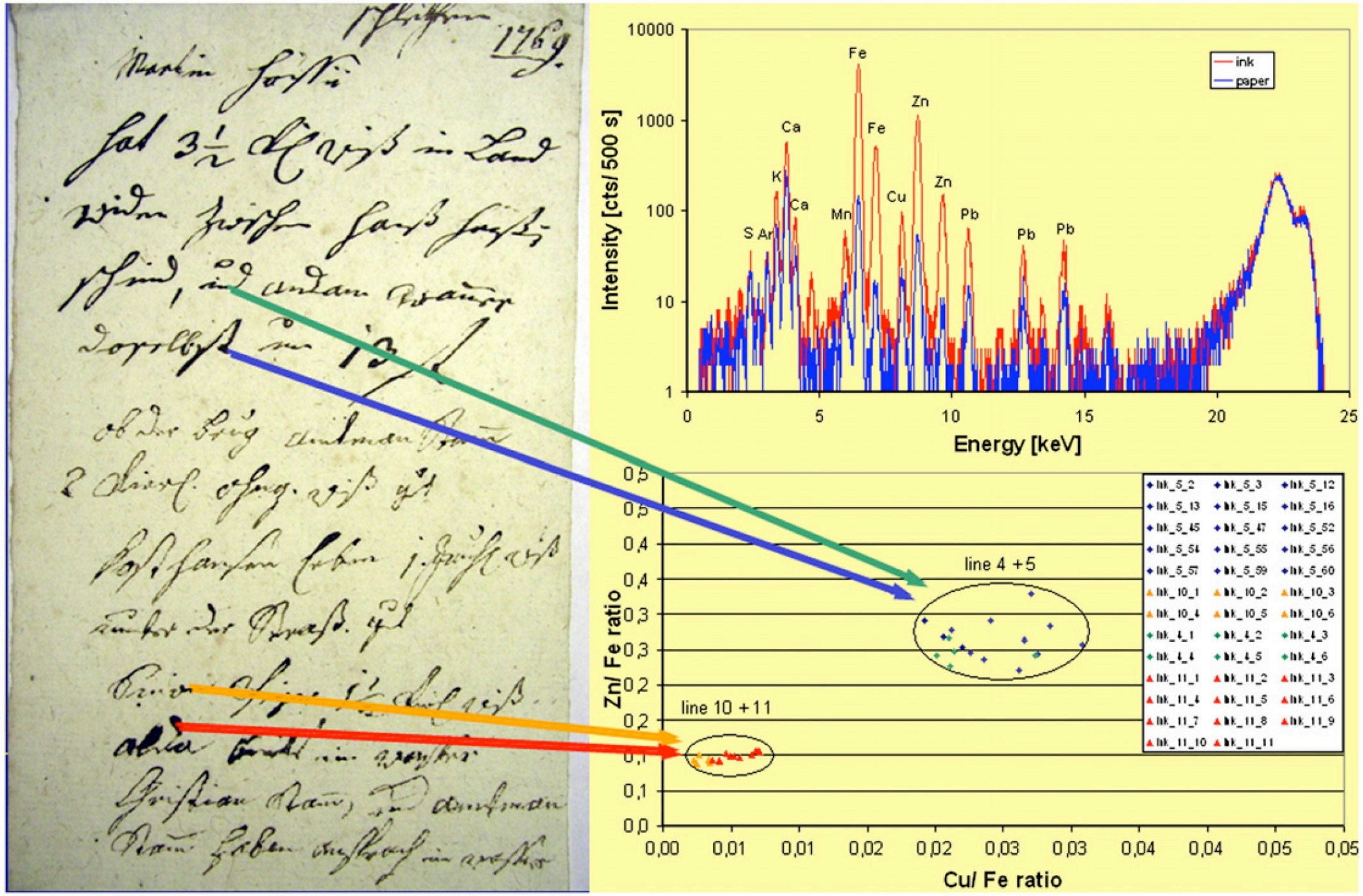

Fig. 4. Photo of the manuscript; right top: representative SR-μXRF spectra (21.5 keV excitation energy, 20 μm capillary, measuring time: 500 s) of the iron gall ink and paper; right bottom: zinc to copper ratio of iron gall ink in different lines of the manuscript.

Archaeological and cultural heritage

Faubel et al. (2007)

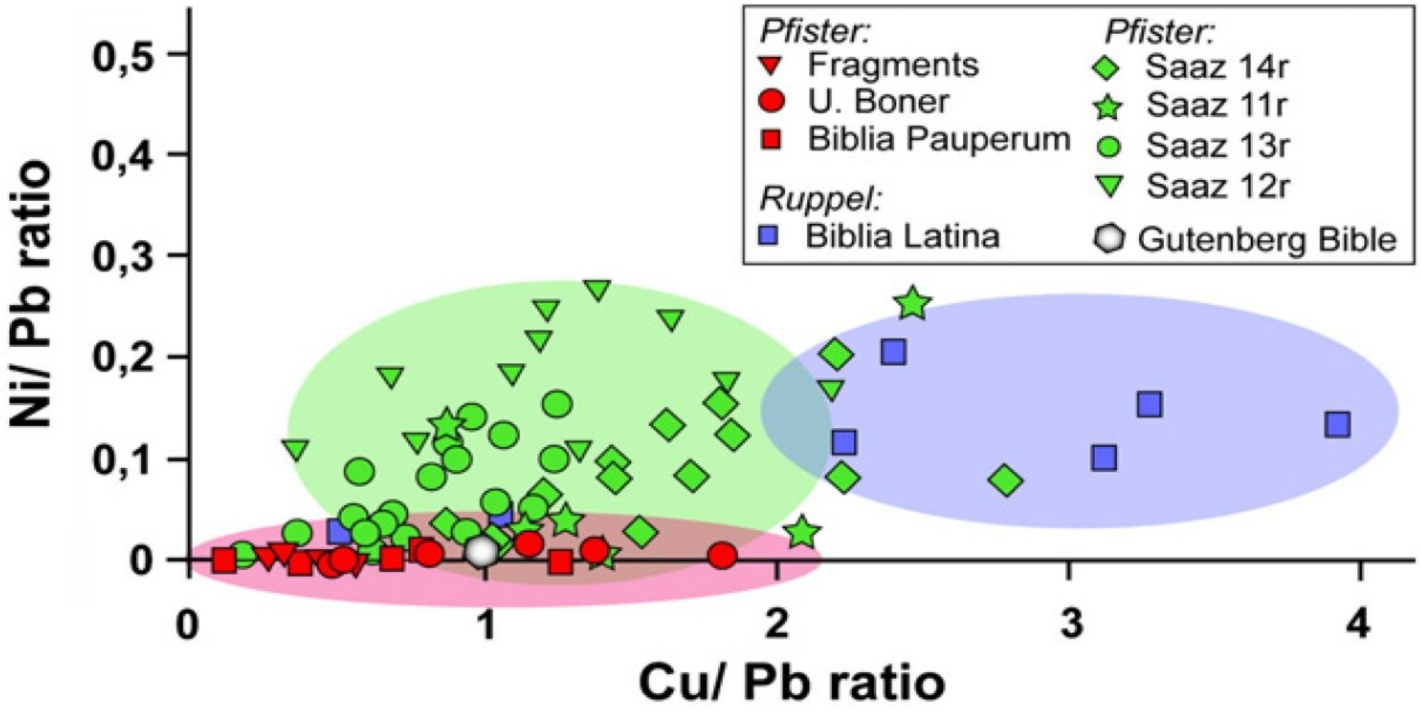

Fig. 11. Analysis of different papers of incunabula of the 15th century from Albrecht Pfister, Bamberg, and other printers as B. Ruppel, Basel, from the same period.

Our Goal: Operational X-ray microprobe in Autumn 2010

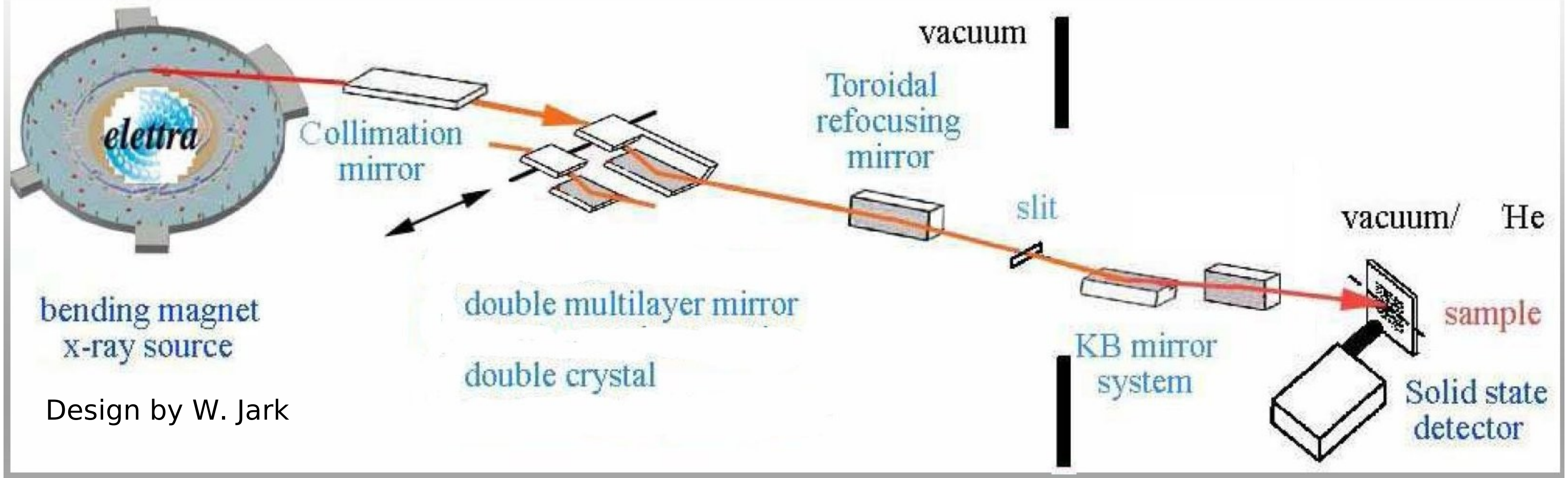

Energy ~ 2 to 14 keV, P to As K_{abs} , Rb to Pt L_{abs}

Focal spot ~ 1 x 1 μm (the smaller the better)

Flux > 10^9 photons/s/0.01% bandwidth

Source to sample: 29 m, Detection limit ~ 1ppm

Thank you very much for your attention

Liping Bai at GSECARS, APS

GSECARS with WDS

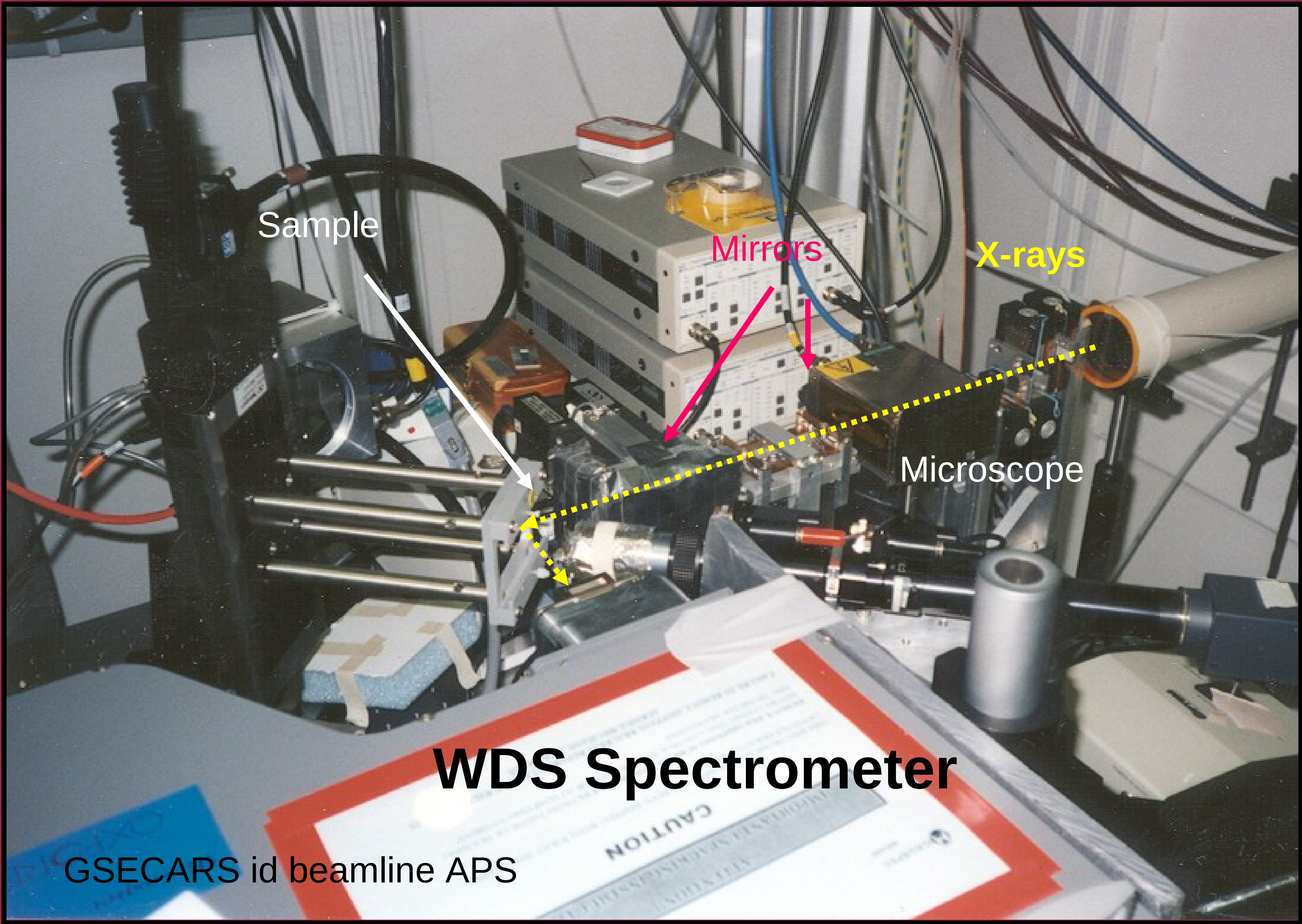

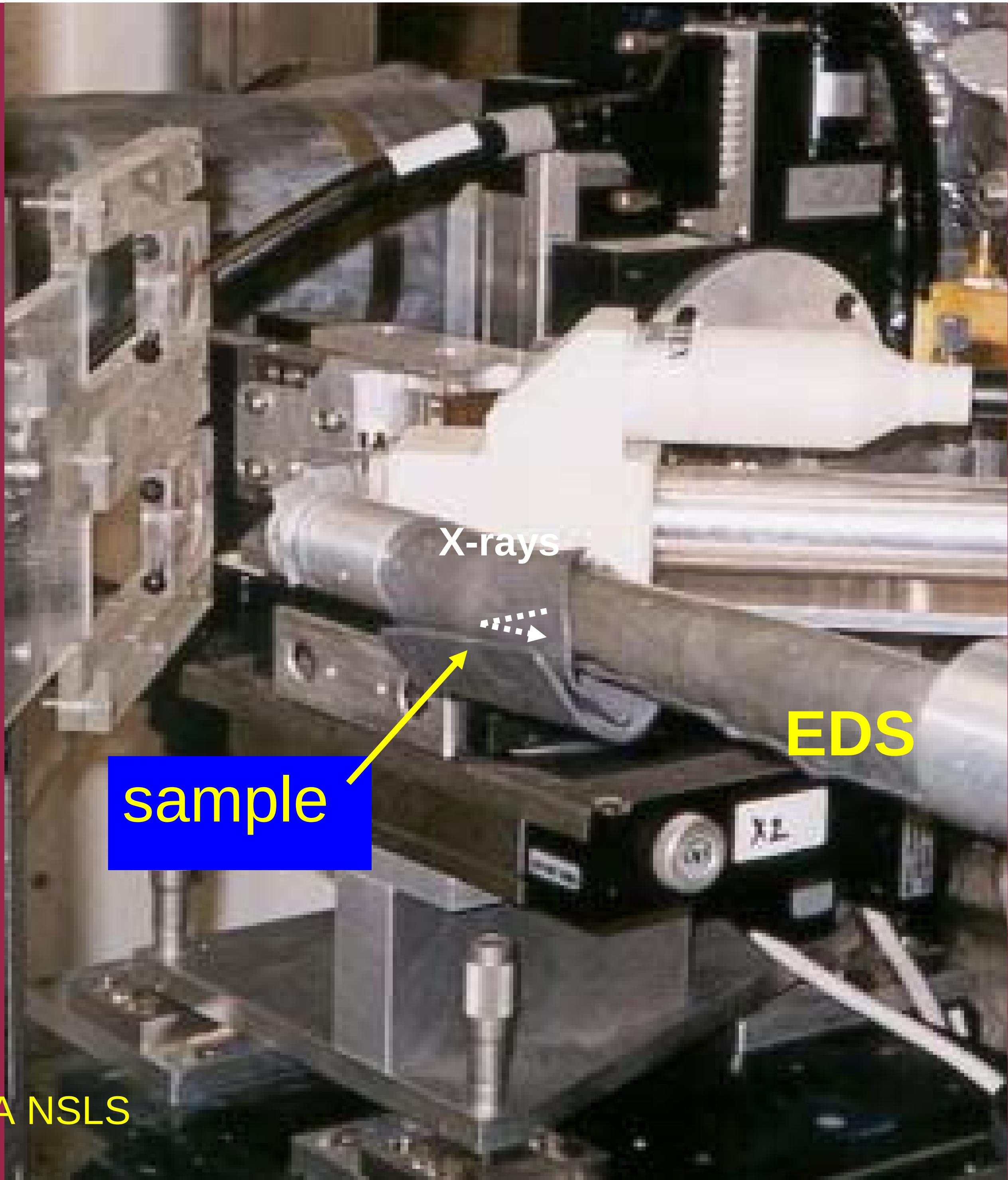

X-26A NSLS